NeuroImage: Clinical 20 (2018) 1176–1190

Contents lists available at ScienceDirect

NeuroImage: Clinical

journal homepage: www.elsevier.com/locate/ynicl

Selective modulation of brain network dynamics by seizure therapy in treatment-resistant depression

Sravya Atluri[a,b], Willy Wong[b,c], Sylvain Moreno[d], Daniel M. Blumberger[a,e,f], Zafiris J. Daskalakis[a,e,f], Faranak Farzan[a,e,f,g,*]

[a] Centre for Addiction and Mental Health, 1001 Queen St. W, Toronto, ON M6J 1A8, Canada
[b] Institute of Biomaterials and Biomedical Engineering, University of Toronto, Rosebrugh Building, Room 407, 164 College St, Toronto, ON M5S 3G9, Canada
[c] The Edward S. Rogers Sr. Department of Electrical & Computer Engineering, University of Toronto, 10 King's College Road, Toronto, ON M5S 3G4, Canada
[d] School of Interactive Art and Technology, Simon Fraser University, 250-13450 102 avenue, Surrey, BC V3T 0A3, Canada
[e] Department of Psychiatry, University of Toronto, 250 College Street, 8th floor, Toronto, ON M5T 1R8, Canada
[f] Institute of Medical Science, Faculty of Medicine, University of Toronto, Medical Sciences Building, 1 King's College Circle, Toronto, ON M5S 1A8, Canada
[g] School of Mechatronic Systems Engineering, Simon Fraser University, 250-13450 102 avenue, Surrey, BC V3T 0A3, Canada

ARTICLE INFO

Keywords:
Microstate analysis
Network dynamics
Treatment-resistant depression
Electroconvulsive therapy
Magnetic seizure therapy
Electroencephalography

ABSTRACT

Background: Electroconvulsive therapy (ECT) is highly effective for treatment-resistant depression, yet its mechanism of action is still unclear. Understanding the mechanism of action of ECT can advance the optimization of magnetic seizure therapy (MST) towards higher efficacy and less cognitive impairment. Given the neuroimaging evidence for disrupted resting-state network dynamics in depression, we investigated whether seizure therapy (ECT and MST) selectively modifies brain network dynamics for therapeutic efficacy.

Methods: EEG microstate analysis was used to evaluate resting-state network dynamics in patients at baseline and following seizure therapy, and in healthy controls. Microstate analysis defined four classes of brain states (labelled A, B, C, D). Source localization identified the brain regions associated with these states.

Results: An increase in duration and decrease in frequency of microstates was specific to responders of seizure therapy. Significant changes in the dynamics of States A, C and D were observed and predicted seizure therapy outcome (specifically ECT). Relative change in the duration of States C and D was shown to be a strong predictor of ECT response. Source localization partly associated C and D to the salience and frontoparietal networks, argued to be impaired in depression. An increase in duration and decrease in frequency of microstates was also observed following MST, however it was not specific to responders.

Conclusion: This study presents the first evidence for the modulation of global brain network dynamics by seizure therapy. Successful seizure therapy was shown to selectively modulate network dynamics for therapeutic efficacy.

1. Introduction

Over one third of patients with major depressive disorder are treatment-resistant and fail to respond to two or more antidepressant medications or psychotherapy (Fava, 2003; Berlim and Turecki, 2007). This trial-and-error approach can be overbearing for patients in terms of cost, as well as the emotional trauma associated with the prolonged treatment process (Fekadu et al., 2009). Such cases of treatment-resistant depression are also challenging for clinicians. Through the process of identifying an optimal treatment, patients may receive several courses of medication and each treatment course can significantly impact brain circuitry, regardless of clinical outcome (Fu et al., 2013; Mayberg et al., 1997; Mayberg, 2003; Kennedy et al., 2001). The complexity of these individual differences can further complicate the

Abbreviations: TRD, Treatment-resistant depression; ECT, Electroconvulsive therapy; MST, Magnetic seizure therapy; EEG, Electroencephalogram; fMRI, Functional magnetic resonance imaging; RUL-UB, Right unilateral ultra-brief; BL, Bitemporal brief pulse; HRSD, Hamilton rating scale for depression; MoCA, Montreal cognitive assessment; MADRS, Montgomery-asberg depression rating scale; BDI, Beck's depression inventory; SSI, Scale for suicidal ideation; ROC, Receiver operating characteristic curve; AUC, Area under the curve

* Corresponding author at: School of Mechatronic Systems Engineering, Simon Fraser University, 250-13450 102 Avenue, Room 4138, Surrey, BC V3T 0A3, Canada.
E-mail address: ffarzan@sfu.ca (F. Farzan).

https://doi.org/10.1016/j.nicl.2018.10.015
Received 19 February 2018; Received in revised form 1 October 2018; Accepted 16 October 2018
Available online 17 October 2018

process of identifying an appropriate treatment for these patients. To date, electroconvulsive therapy (ECT) remains the most effective treatment for patients with treatment-resistant depression (Heijnen et al., 2010; Kho et al., 2003). Yet its mechanism of action is still not known.

It is hypothesized that the brief, generalized seizure triggered by ECT impacts the dynamics of brain networks disrupted in depression (Farzan et al., 2014) but also networks involved in cognition, leading to its most common adverse effect: memory impairment (Devanand et al., 1995). Magnetic seizure therapy (MST) (Lisanby et al., 2003) also relies on the principles of seizure induction for therapeutic benefit but unlike ECT, the effect of MST is localized (Deng et al., 2011). Based on the few clinical trials conducted to date, MST improves depressive symptoms (Kayser et al., 2011; Kayser et al., 2015; Cretaz et al., 2015) and suicidal ideation (Sun et al., 2016), without the cognitive side effects seen with ECT (Lisanby et al., 2003; Deng et al., 2015; Spellman et al., 2008; Moscrip et al., 2006). However, in its early stage of development, its efficacy relative to ECT requires further study (Kayser et al., 2011). Identifying brain networks affected by treatment-resistant depression and modified by ECT may allow the optimization of MST as well as the development of non-invasive and non-seizure inducing treatments.

Evidence from neuroimaging studies suggests that specific patterns of brain network dysfunction at rest may contribute to core deficits in cognitive and affective functions underlying neuropsychiatric disorders (Bassett and Bullmore, 2006; Garrity et al., 2007; Greicius, 2008; Buckner et al., 2009; Wang et al., 2009; Zhang et al., 2011). It has also been shown that the resting-state of the brain can predict physiological consequences of brain stimulation and treatment outcome (Mayberg, 2003; Fox et al., 2014; Greicius et al., 2007). Collectively, the temporal variation in resting-state brain network dynamics may be a significant marker of illness and therapeutic outcome (Hutchison et al., 2013; Chang and Glover, 2010; Honey et al., 2007). To advance the development of novel and targeted treatments, it is critical to characterize the disruption and changes in brain network dynamics in treatment-resistant depression and by successful treatments such as ECT (Abbott et al., 2014; Nobler et al., 2001; Perrin et al., 2012).

Using electroencephalography (EEG), functional brain networks and their dynamics can be examined through microstate analysis, a data-driven approach used to measure the spatial stability of brain network dynamics over time (Lehmann et al., 1987; Pascual-Marqui et al., 1995; Michel and Koenig, 2017). Microstate analysis clusters the topographical distributions of spontaneous EEG activity into a set of four classes (A, B, C and D as described in the method) of brain states (i.e., microstates) that each remain stable over a short period of time before transiting into another state (50–120 ms) (Strik et al., 1995). An increase in the duration of a microstate implies an increase in the probability of that microstate to be followed by itself. Since each microstate is generated by an underlying neuronal population, the temporal characteristics of a microstate (such as rate of change or duration) may be considered as an expression of the dynamic stability of underlying spatial networks (Brodbeck et al., 2012). The duration of microstates is also consistent with the duration of high-level cognitive processes, as shown by evoked-potential studies (Kok, 1997). Moreover, microstates were shown to be state-dependent, to vary across age, cognitive state (Brodbeck et al., 2012; Koenig et al., 2002; Milz et al., 2016a; Santarnecchi et al., 2017) and in response to therapy (Kinoshita et al., 1995; Rodriguez et al., 2002; Kikuchi et al., 2007). Studies have also confirmed the reliability of microstates across repeated testing sessions (Khanna et al., 2014).

Microstates were previously linked with brain networks identified through resting-state functional magnetic resonance imaging (fMRI) (Britz et al., 2010; Musso et al., 2010; Yuan et al., 2012), some suggested to be impaired in depression (Kaiser et al., 2015; Fischer et al., 2016; Veer et al., 2010; Whitfield-Gabrieli and Ford, 2012). For example, microstates C and D were linked to the salience and frontoparietal networks (Britz et al., 2010) and the relative activation of these networks is hypothesized to be impaired in depression (Mulders et al., 2015; Hamilton et al., 2011). However, to date, there has been only one study that examined and reported a decrease in duration of microstates in depression compared to healthy controls (Strik et al., 1995). This study was not in treatment-resistant patients and may not extend to treatment-resistant depression (Yamamura et al., 2016; de Kwaasteniet et al., 2015; Wu et al., 2011; Guo et al., 2011).

Collectively, the evidence in support of resting-state network abnormalities in depression (Kaiser et al., 2015; Fischer et al., 2016; Veer et al., 2010; Whitfield-Gabrieli and Ford, 2012), the sensitivity of microstates in detecting intervention-related changes in resting-state networks (Kinoshita et al., 1995; Rodriguez et al., 2002; Kikuchi et al., 2007), and the consistency of microstates across repeated testing sessions (Khanna et al., 2014), motivated the utility of EEG microstates in this study. Using the high temporal resolution of EEG to an advantage, we aimed to investigate the therapeutic impact of seizure therapy on network dynamics and the temporal stability of brain network dynamics between patients with treatment-resistant depression and healthy subjects.

Our primary hypotheses were two-fold: (a) microstates C and D, previously associated with the salience and frontoparietal networks implicated in depression, will be modulated by successful seizure therapy; (b) baseline and seizure therapy-induced changes in microstates will be associated with therapeutic outcome, and could explain changes in cognition and suicidal ideation. Our secondary hypothesis was that patients with treatment-resistant depression will present different microstate dynamics compared to healthy controls. These dynamics will be modulated by seizure therapy towards the healthy group dynamics.

2. Material and methods

2.1. Subjects

Data was collected from 75 patients (Age: $\mu = 45.7$, $\sigma = 14.4$; 44 females) with a Structured Clinical Interview for the Diagnostic and Statistical Manual of mental disorders (DSM-IV) diagnosis of Major Depressive Disorder who previously did not respond to 2 or more antidepressants (i.e., treatment-resistant depression), and 55 healthy controls (Age: $\mu = 39.2$, $\sigma = 17.4$; 29 females) with written informed consent. Of the 75 patients, follow-up assessments were conducted for 22 patients receiving ECT and 24 receiving MST. The remaining 29 patients either did not provide their consent for follow-up or withdrew from the study. There were no significant differences in clinical scores, age or sex between the group of patients that did the follow-up assessment and the group of patients that did not.

2.2. Seizure therapy

ECT was administered with spectrum 500Q (MECTA Corporation) according to standards of practice (Sackeim et al., 2008). Of the 22 patients who completed ECT treatment, 14 patients received right unilateral ultra-brief (RUL-UB) pulse width ECT, 2 received bitemporal brief pulse (BL) ECT and the rest (6 patients) started on RUL-UB and then switched to BL ECT due to the lack of efficacy. Treatments were administered 2–3 times a week and continued until patients were in remission or improvement plateaued. MST was administered using the MagPro MST using a Twin Coil (MagVenture). The centre of each circular coil was placed over F3 and F4 respectively, using the international 10–20 system for EEG electrode placement. The highest electric field strength roughly corresponds to Fz (Deng et al., 2013) or the dorsomedial prefrontal cortex. Of the 24 patients who received MST, 12 patients received 100 Hz MST, 1 patient received 60 Hz, 2 received 50 Hz and 9 received 25 Hz. Treatments were administered 2–3 times per week until remission or up to a maximum of 24 sessions. Please see Table 1 for additional details.

Table 1
Clinical data table.

	TRD	*n*	ECT Pre + Post	*n*	MST Pre + Post	*n*
Demographic Characteristics						
Age, years: mean (std)	45.7 (14.4)	75	46.8 (15.8)	22	42.0 (13.4)	24
Sex, M/F	31/44	75	8/14	22	12/12	24
Clinical Characteristics						
Illness Duration: mean (std)	20.3 (13.2)	74	19.0 (12.0)	22	20.3 (13.7)	24
On Medications (Antidepressants or Benzodiazepines) (Yes/No)	60/10	70	20/2	22	20/4	24
Avg. No. of Treatment Sessions: mean (std)	–	–	14.2 (5.2)	22	20.2 (6.19)	24
Site of Treatment [a]	–	–	RUL UB	14	DMPFC	24
			RUL UB then BL	6		
			BL	2		
Stimulation Frequency: [a]	–	–	–	–	100 Hz	12
					60 Hz	1
					50 Hz	2
					25 Hz	9
Clinical Assessments						
HRSD, % change following Seizure Therapy: mean (std)	36.7 (30.0)	46	44.8 (28.6)	22	29.3 (29.9)	24
Initial HRSD scores, mean(std)	26.6 (4.44)	74	24.5 (3.81)	22	28.1 (4.73)	24
Post HRSD scores, mean(std)	–	–	13.0 (6.19)	22	19.3 (7.96)	24
HRSD, Responders/Nonresponders [b]	20/26	46	13/9	22	7/17	24
MoCA, change following seizure therapy: mean (std)	0.56 (3.32)	46	–3 (2.97)	6	1.57 (2.69)	21
MoCA: # patients with improvement > 0	12	27	0	6	12	21
BDI, % change: mean (std)	–	–	49.2 (31.2)	17	–	–
BDI, Responders/Nonresponders [b]	–	–	9/8	17	–	–
MADRS, % change: mean (std)	–	–	50.0 (32.6)	18	–	–
MADRS, Responders, Nonresponders [b]	–	–	11/7	18	–	–
SSI, change: mean (std)	–	–	–	–	6.4 (6.4)	20
SSI, Responders/Nonresponders [b]	–	–	–	–	16/4	20

TRD: Treatment-Resistant Depression; ECT: electroconvulsive therapy; MST: magnetic seizure therapy.
[a] RUL UB: Right Unilateral Ultra-Brief Pulse Width; BL: Bitemporal (brief pulse width); DMPFC: Dorsomedial Prefrontal Cortex.
[b] Response for HRSD/BDI/MADRS/SSI defined as ≥ 50% improvement in score.

2.3. Clinical assessments

Prior to and following a course of ECT, the 17-scale Hamilton Rating Scale for Depression (HRSD) and Montreal Cognitive Assessment (MoCA) v7.1–7.3 were used to clinically assess severity of depression and global cognition. Montgomery-Åsberg Depression Rating Scale (MADRS) and Beck's Depression Inventory (BDI-II) scale were also used to assess clinical severity of depression and self-rated depression symptoms, respectively. Prior to and following a course of MST, the 24-scale HRSD and Montreal Cognitive Assessment (MoCA) v7.1–7.3 were used to clinically assess severity of depression and global cognition. Severity of suicidal thoughts and overall risk for suicide was assessed using the Scale for Suicidal Ideation (SSI). For all SSI-related analyses, only participants who showed suicidal ideation at baseline were included. The criterion for treatment response was a minimum of 50% improvement in HRSD (final scores were < 17). Response for BDI, MADRS and SSI was also defined as a minimum of 50% improvement in score. Demographic and clinical characteristics are presented in Table 1.

2.4. Data recording and pre-processing

Eyes-closed rest EEG data was collected within a week prior to the first treatment session and again within 2 weeks after the completion of the last treatment. Data was recorded with the Compumedics (Charlotte, NC, USA) Neuroscan SynAmps 2/RT 64-channel EEG system at 10 kHz. During pre-processing, EEG data was downsampled to 1000 Hz, divided into 2-s epochs, bandpass-filtered between 1 and 80 Hz, and notch-filtered at 60 Hz. With the removal of eye electrodes and other unused channels, the total number of EEG channels used for analysis was 60. Using EEGLAB (Delorme and Makeig, 2004), independent component analysis was used to extract eye, muscle and electrode artifacts. Deleted EEG channels were interpolated using spherical spline interpolation (Perrin et al., 1989) and data was re-referenced to an average reference. This preprocessing pipeline is currently made available as ERPEEG (http://www.tmseeg.com/multisiteprojects/). Channels were deleted if: (i) they were disconnected during collection for a significant amount of the data collection time (> 40%), or (ii) heavily contaminated with noise (muscle or spurious artifacts) for a significant part of the data collection time (> 40%). On average, 6 ± 3 independent components were removed and 3 ± 1 channels were deleted and interpolated in the data collected from healthy subjects. In the data collected from patients at baseline, 9 ± 5 independent components were removed and 3 ± 1 channels were deleted and interpolated. In the data collected from patients following treatment, 10 ± 5 independent components were removed and 3 ± 2 channels were deleted and interpolated.

2.5. Microstate analysis

Microstate analysis followed the standard procedure outlined in seminal work (Fig. S1) (Lehmann et al., 1987; Pascual-Marqui et al., 1995) and was implemented using CARTOOL (Brunet et al., 2011). Prior to the application of microstate analysis, four minutes of the pre-processed EEG data was bandpass-filtered from 1 to 30 Hz.

Global field power is a measure of the electric field strength over the scalp and is defined as the variance in electrical activity across EEG electrodes at each time point (Eq. (1)). The topographical maps at the local maxima peaks of the global field power curve are clustered to derive the four prototypical microstate classes (Koenig et al., 2002). Using a data-driven approach, the optimal number of clusters for the data used in this study was found to be four (Fig. S2).

$$GFP(t) = \sqrt{\frac{\left[\sum_i^N \left(V_i(t) - V_{mean}(t)\right)\right]^2}{N}} \quad (1)$$

where N represents the number of EEG electrodes (i = 1:60 electrodes) and v represents the electrical potential measured over the scalp. In addition, v_i represents the electrical potential measured at electrode (i) and time (t), and v_{mean} represents the average electrical potential over

all electrodes at time (t).

In this study, the topographical atomize–agglomerate hierarchical clustering algorithm(Tibshirani and Walther, 2005) was applied across all subjects and conditions (global approach). By recalculating microstate classes for each subject or condition, minor differences may be introduced in the microstate topographies. The global clustering approach provides low within-subject error and high test-retest reliability in resting-state microstate analysis (Khanna et al., 2014). Clustered microstates were labelled A, B, C and D as seen in seminal work (Koenig et al., 2002) and explained 83% of variance in our data. In the final step, topographical maps at each local maxima point of the global field power curve were assigned to the microstate class of highest correlation using spatial Pearson's product-moment correlation coefficient (Eq. (2)) (Brandeis et al., 1992). Three features were calculated for each of the four microstate classes: (i) average duration, (ii) frequency, and (iii) coverage. Average duration is the amount of time a microstate class remains stable when it appears, in milliseconds; frequency refers to the occurrence of each microstate class per second; and coverage is the percent of recording covered by each microstate class.

$$r_{spatial} = 1 - \frac{1}{2}\left[\frac{1}{N}\sum_{i=1}^{N}\left\{\frac{u_i - u_{mean}}{\sqrt{\sum_{i=1}^{N}(u_i - u_{mean})^2/N}} - \frac{v_i - v_{mean}}{\sqrt{\sum_{i=1}^{N}(v_i - v_{mean})^2/N}}\right\}^2\right] \quad (2)$$

where N represents the number of EEG electrodes (i = 1:60 electrodes) and u and v represent the 2 different spatial topographies (maps) being correlated. In addition, u_i, v_i represent the electrical potential measured at electrode i of the 2 maps and u_{mean}, v_{mean} represent the average electric potential over all electrodes.

2.6. Statistical analysis

To examine the effect of treatment response (≥50% improvement in HRSD) on microstate characteristics following seizure therapy (ECT and MST), a 2 × 2 × 4 repeated-measures ANOVA (Lehmann et al., 2005; Tomescu et al., 2014) was conducted for each microstate feature (Duration, Frequency and Coverage) with *RESPONSE* (Responder, Non-responder) as a categorical factor, and *TIME* (Pre, Post) and *MICROSTATE CLASS* (A, B, C, D) as the repeated-measures factors. These ANOVAs were performed on the ECT and MST group data separately as well.

For each microstate feature (Duration, Frequency and Coverage), a 2 × 4 repeated-measured ANCOVA (Lehmann et al., 2005; Tomescu et al., 2014) was conducted between (2 *GROUPS*) healthy controls and patients with treatment-resistant depression prior to seizure therapy using *MICROSTATE CLASS* (A, B, C and D) as the repeated-measure. For each of the three microstate features, an ANCOVA was performed again between (2 *GROUPS)* healthy controls and patients following seizure therapy using *MICROSTATE CLASS* (A, B, C and D) as the repeated-measure. Age was used as a covariate. There were no significant effects of gender.

Based on our hypothesis that seizure therapy modulates global neural dynamics, planned comparisons were performed to determine whether changes in microstate characteristics were associated with treatment response. For each of the three microstate characteristics (duration, frequency, coverage), paired t-tests were performed to compare the characteristic before and after treatment for each of the four states. The results were corrected for multiple comparisons using the Bonferroni correction method (for the 4 microstates).

A significance level of $\alpha < 0.05$ was used for all statistical tests. Pairwise post-hoc comparisons were performed using Tukey-HSD. All planned comparisons were corrected using the Bonferroni method (4 comparisons for the 4 microstate classes).

2.7. Correlation and predictive analysis

Associations between microstate characteristics and clinical assessments (HRSD, MADRS, BDI, MoCA, SSI) were evaluated with a non-parametric spearman rank-order correlation test and corrected for multiple-comparisons using permutation tests. Receiver operating characteristic (ROC) curves were used to assess predictive value of significant spearman rank-order correlations (i.e., correlations with $p < 0.05$). Significance of prediction for the ROC curves was quantified through area under the curve (AUC). Only AUC values greater than or equal to 0.7 (i.e., fair, good or excellent predictors) are reported in this manuscript. For ROC curves with HRSD, MADRS or BDI, subjects were grouped to be responders (≥ 50% improvement in symptoms) or non-responders. For ROC curves with MoCA, subjects were grouped to have cognitive decline if the percent change in MoCA was negative.

Microstate features were correlated with the percent change in clinical scores following therapy. Raw clinical scores (e.g., HRSD) were not used for correlation analysis. Change in microstate features was calculated as (Post-Pre)/Pre*100 where a higher percentage represents an increase in the feature value; change in HRSD, MADRS and BDI were calculated as (Pre-Post)/Pre*100 where a higher percentage represents improvement in depressive symptoms; and lastly change in MoCA and SSI were calculated as (Post-Pre) where a higher value represents improvement in cognition or suicidal ideation symptoms.

2.8. Source localization

The eLORETA algorithm was used to localize the four global-clustered microstates in the source domain. Using LORETA-KEY (Pascual-Marqui et al., 1999), the co-ordinates of the 60 electrodes were identified according to the 10–10 system. A transformation matrix (60 × 6239) was then derived with a relative regularization parameter of 1.

2.9. Power spectral density analysis

The EEGLAB function *spectopo* was used to obtain the power spectrum for each electrode. Relative power was obtained for 1 to 30 Hz (to be consistent with microstate analysis) and was calculated as the ratio of the power at each frequency relative to the sum of power across all frequencies. In addition, relative power was calculated as an average over the following bands: Delta: 1–4 Hz; Theta: 4–8 Hz; Alpha: 8–14 Hz; Low Beta: 14–20 Hz; High Beta: 20–30 Hz. Spearman rank-order correlations were performed between power in each band and the characteristics of microstate analysis (duration, frequency and coverage). The results are reported as a correlation matrix. Correlation p-values were also calculated and were Bonferroni-corrected for multiple comparisons (12 comparisons: 4 microstate classes by 3 features).

3. Results

A significant improvement in HRSD score was observed following ECT (paired $t = -6.6$; $df = 21$; $p < 0.0001$; Cohen's $d = 2.2$), following MST (paired $t = -4.62$, $df = 23$; $p = 0.0001$; Cohen's $d = 1.3$) and when both the groups were combined as seizure therapy (paired $t = -7.8$, $df = 45$; $p < 0.0001$; Cohen's $d = 1.6$). In addition, there was a significant improvement in BDI score (paired $t = -5.8$, $df = 16$; $p < 0.0001$; Cohen's $d = 1.9$) and a decrease in MoCA score (cognition) approaching significance (paired $t = -2.5$; $df = 5$; $p = 0.05$; Cohen's $d = 1.2$) following ECT. Suicidal ideation (paired $t = -4.5$, $df = 19$; $p = 0.0002$; Cohen's $d = 1.3$) and cognition scores (paired $t = 2.7$, $df = 20$; $p = 0.01$; Cohen's $d = 0.48$) significantly changed following MST.

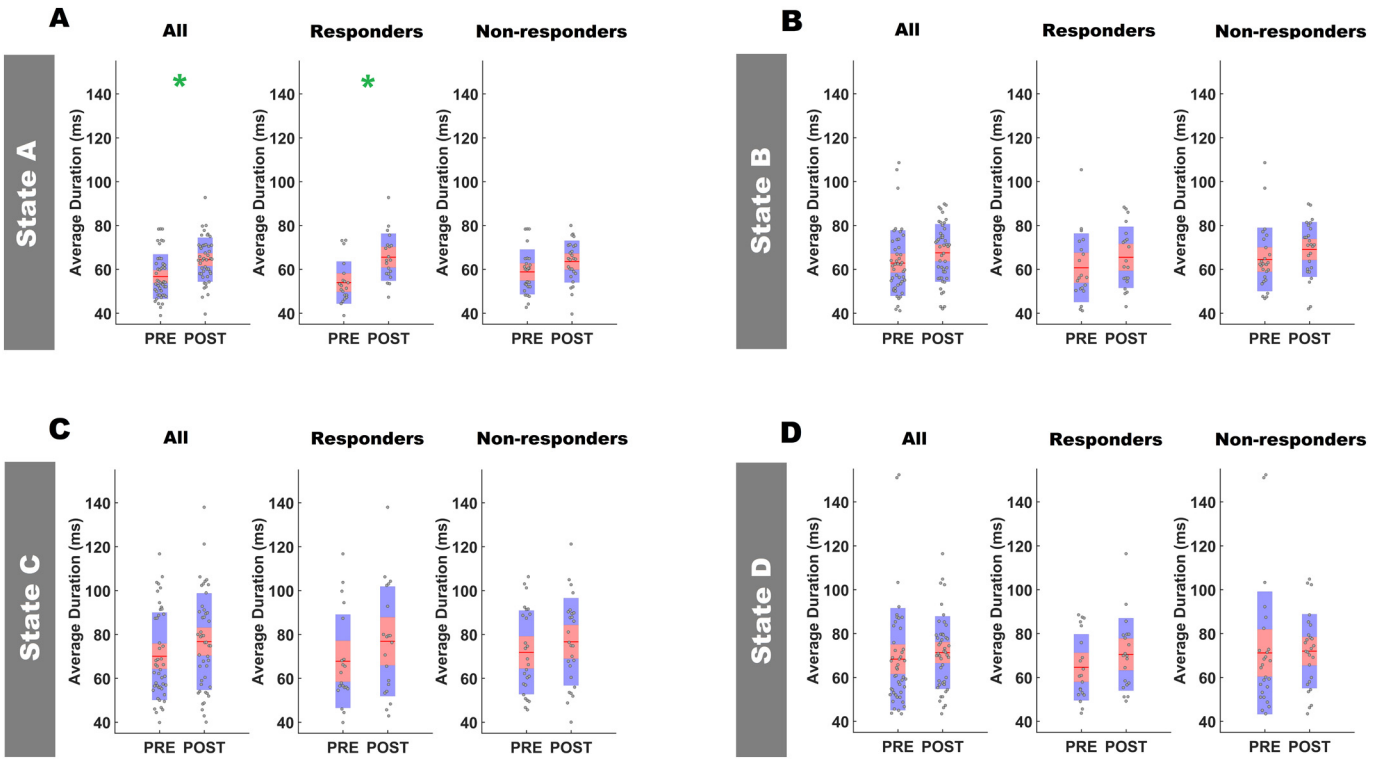

Fig. 1. Effect of seizure therapy (ECT and MST) on the average duration of all four microstates. In each subplot, the raw data is plotted on top of a boxplot showing the mean (red line), 95% confidence interval (red area) and 1 standard deviation (blue area). Significant comparisons are marked with a green (*). **(A) Left panel:** Following seizure therapy (ECT and MST), there was a significant increase in the duration of State A (y-axis) ($p < 0.0001$). **Middle and right panels:** This increase was specific to responders of seizure therapy ($p < 0.0001$). **(B)** No significant changes were observed in the duration of State B. **(C)** No significant changes were observed in the duration of State C. **(D)** No significant changes were observed in the duration of State D.

3.1. Effect of seizure therapy on EEG microstate dynamics

3.1.1. Seizure therapy (ECT and MST)

A main effect of *Time* (F = 15.9; *df* = 1,44; $p = 0.0003$; $\eta_p^2 = 0.27$) and *Microstate Class* (F = 13.2; *df* = 3,132; $p < 0.0001$; $\eta_p^2 = 0.23$) were observed in the duration of microstates. The interaction of *Time* × *Microstate Class* was not significant (F = 1.2; *df* = 3,132; $p = 0.3$; $\eta_p^2 = 0.026$). An effect of *response* (≥50% improvement in HRSD) was not observed (F = 0.57; *df* = 1,44; $p = 0.5$; $\eta_p^2 = 0.013$). Since all the states increased in duration following seizure therapy (ranging between 3.3 to 8.2 ms), paired *t*-tests were performed to identify which states revealed a statistically significant increase in duration. These were corrected using the Bonferroni method for 4 comparisons (4 microstates). State A (paired $t = 5.0$; *df* = 45; *Bonferroni-corrected* $p < 0.0001$; Cohen's $d = 0.77$) showed a significant increase in duration following seizure therapy (left panel of Fig. 1A). There was no significant change in the duration of State B (paired $t = 2.4$; *df* = 45; *Bonferroni-corrected* $p = 0.08$; Cohen's $d = 0.33$), State C (paired $t = 2.2$; *df* = 45; *Bonferroni-corrected* $p = 0.1$; Cohen's $d = 0.32$), or State D (paired $t = 1.4$; *df* = 45; *Bonferroni-corrected* $p = 0.7$; Cohen's $d = 0.15$) (left panels of Fig. 1B–D).

A main effect of *Time* (F = 12.4; *df* = 1,44; $p = 0.001$; $\eta_p^2 = 0.22$) and *Microstate Class* (F = 3.5; *df* = 3,132; $p = 0.02$; $\eta_p^2 = 0.07$) was observed in the frequency of microstates. The interaction of *Time* × *Microstate Class* approached significance (F = 2.4; *df* = 3,132; $p = 0.06$; $\eta_p^2 = 0.052$). Post-hoc Tukey-HSD tests revealed that State B (HSD = 4.7; *df* = 132; $p = 0.03$; Cohen's $d = 0.65$) (left panel of Fig. 2B), State C (HSD = 5.6; *df* = 132; $p = 0.004$; Cohen's $d = 0.78$) (left panel of Fig. 2C) and State D (HSD = 6.2; *df* = 132; $p = 0.0008$; Cohen's $d = 0.87$) (left panel of Fig. 2D) *significantly* decreased in frequency following seizure therapy. There was no significant change in the frequency of State A (HSD = 1.3; *df* = 132; $p = 0.99$; Cohen's $d = 0.19$) (left panel of Fig. 2A). An effect of *response* was not observed (F = 0.54; *df* = 1,44; $p = 0.5$; $\eta_p^2 = 0.012$).

Apart from the main effect of *Microstate Class* (F = 8.6; *df* = 3,132; $p < 0.0001$; $\eta_p^2 = 0.16$), no significant effects were observed in the coverage of microstates (Fig. S3).

Planned comparisons were conducted to investigate the effect of response based on our hypotheses. The increase in State A duration was specific to responders of seizure therapy ($t = 6.3$; *df* = 19; $p < 0.0001$; Bonferroni-corrected $p < 0.0001$; Cohen's $d = 1.1$) (middle panel of Fig. 1A). This effect was not observed in non-responders for State A ($t = 2.2$; *df* = 25; $p = 0.03$; Bonferroni-corrected $p = 0.1$; Cohen's $d = 0.48$) (right panel of Fig. 1A). The decrease in frequency of State B ($t = -3.3$; *df* = 19; $p = 0.004$; Bonferroni-corrected $p = 0.01$; Cohen's $d = 0.56$), State C ($t = -4.9$; *df* = 19; $p = 0.0001$; Bonferroni-corrected $p = 0.0004$; Cohen's $d = 0.80$) and State D ($t = -2.8$; *df* = 19; $p = 0.01$; Bonferroni-corrected $p = 0.04$; Cohen's $d = 0.53$) was specific to responders of seizure therapy (middle panels of Fig. 2B–D). This effect was not observed in non-responders for State B ($t = -1.1$; *df* = 25; $p = 0.3$; Cohen's $d = 0.15$), State C ($t = -1.3$; *df* = 25; $p = 0.19$; Cohen's $d = 0.31$) or State D ($t = -1.5$; *df* = 25; $p = 0.2$; Cohen's $d = 0.28$) (right panels of Fig. 2B–D).

3.1.2. Electroconvulsive therapy

A main effect of *Time* (F = 8.3; *df* = 1,20; $p = 0.009$; $\eta_p^2 = 0.29$) and *Microstate Class* (F = 5.9; *df* = 3,60; $p = 0.001$; $\eta_p^2 = 0.23$) was observed in the duration of microstates. The interaction of *Time* × *Microstate Class* was not significant (F = 0.71; *df* = 3,60; $p = 0.6$; $\eta_p^2 = 0.034$). An effect of *response* was not observed (F = 0.002; *df* = 1,20; $p = 0.97$; $\eta_p^2 = 0.00008$). Since all the states increased in duration following ECT (ranging between 6.1 to 11.1 ms), paired *t*-tests were performed to identify which states revealed a statistically significant increase in duration. These were corrected using the Bonferroni

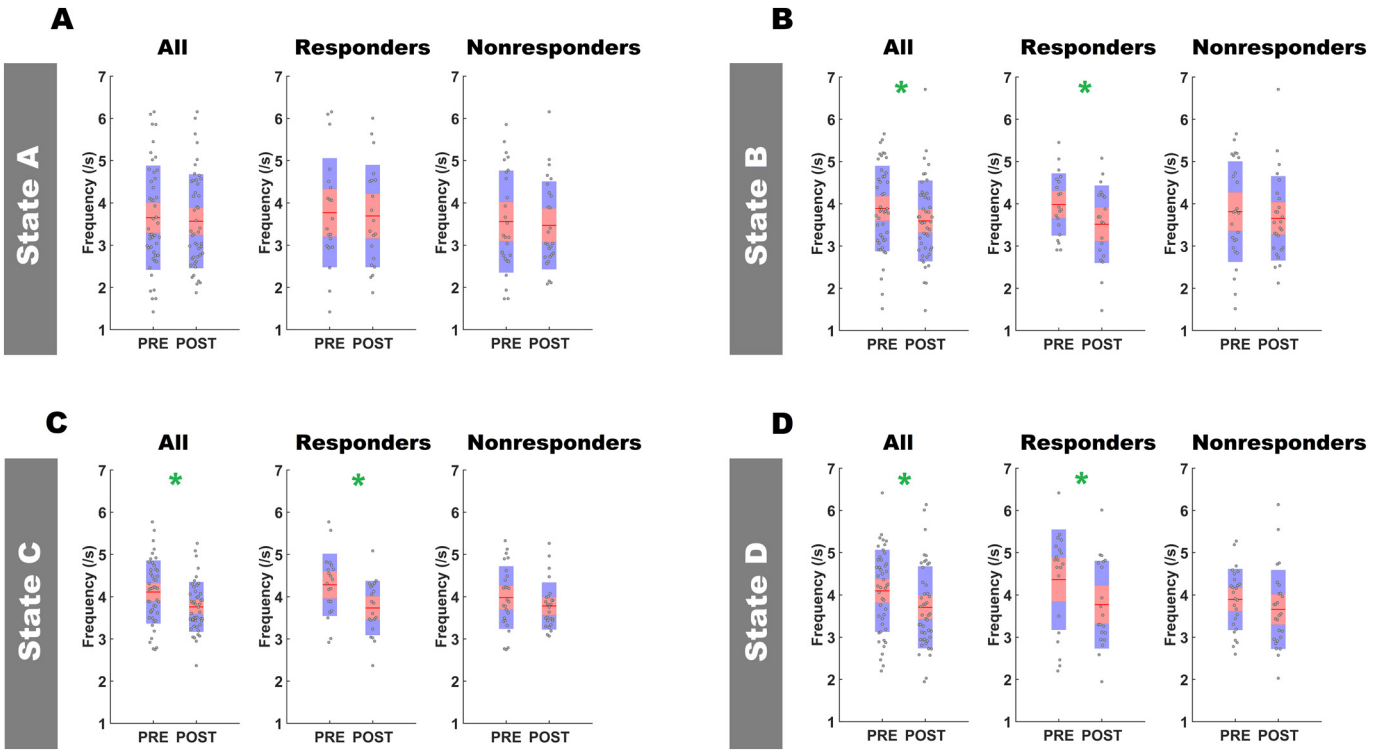

Fig. 2. Effect of seizure therapy (ECT and MST) on the frequency of all four microstates. In each subplot, the raw data is plotted on top of a boxplot showing the mean (red line), 95% confidence interval (red area) and 1 standard deviation (blue area). Significant comparisons are marked with a green (*). **(A)** No significant changes were observed in the frequency of State A. **(B) Left panel:** A decrease in the frequency of State B (y-axis) was observed following seizure therapy ($p = 0.03$). **Middle and right panels:** This decrease in frequency of State B was specific to responders of seizure therapy ($p = 0.01$). **(C) Left panel:** A decrease in the frequency of State C (y-axis) was observed following seizure therapy ($p = 0.004$). **Middle and right panels:** This decrease in frequency of State C was specific to responders of seizure therapy ($p = 0.0004$). **(D) Left panel:** A decrease in the frequency of State D (y-axis) was observed following seizure therapy ($p = 0.0008$). **Middle and right panels:** This decrease in frequency of State D was specific to responders of seizure therapy ($p = 0.04$).

method for 4 comparisons (4 microstates). State A (paired $t = 5.7$; $df = 21$; *Bonferroni-corrected* $p < 0.0001$; Cohen's $d = 1.08$) showed a significant increase in duration following ECT (left panel of Fig. 3A). There was no significant change in the duration of State B (paired $t = 1.7$; $df = 21$; *Bonferroni-corrected* $p = 0.4$; Cohen's $d = 0.36$), State C (paired t = 1.7; $df = 21$; *Bonferroni-corrected* $p = 0.4$; Cohen's $d = 0.43$) or State D (paired $t = 2.3$; $df = 21$; *Bonferroni-corrected* $p = 0.1$; Cohen's $d = 0.35$) (left panels of Fig. 3B–D).

A main effect of *Time* (F = 7.3; $df = 1,20$; $p = 0.01$; $\eta_p^2 = 0.27$), and an interaction effect of *Time* × *Microstate Class* (F = 3.4; $df = 3,60$; $p = 0.02$; $\eta_p^2 = 0.15$) were observed in the frequency of microstates. The main effect of *Microstate Class* was not significant (F = 1.3; $df = 3,60$; $p = 0.3$; $\eta_p^2 = 0.06$). All states decreased in frequency following ECT. Post-hoc Tukey-HSD tests revealed that State B (HSD = 4.4; $df = 60$; $p = 0.03$; Cohen's $d = 1.0$) (left panel of Fig. 4B), State C (HSD = 5.7; $df = 60$; $p = 0.002$; Cohen's $d = 1.24$) (left panel of Fig. 4C) and State D (HSD = 6.6; $df = 60$; $p = 0.0003$; Cohen's $d = 1.46$) (left panel of Fig. 4D) *significantly* decreased in frequency following ECT. There was no significant change in the frequency of State A (HSD = 0.54; $df = 60$; $p = 0.99$; Cohen's $d = 0.11$) (left panel of Fig. 4A). An effect of *response* was not observed (F = 0.04; $df = 1,20$; $p = 0.8$; $\eta_p^2 = 0.002$).

Apart from the main effect of *Microstate Class* (F = 3.1; $df = 3,60$; $p = 0.03$; $\eta_p^2 = 0.13$), no significant effects were observed in the coverage of microstates (Fig. S4).

Planned comparisons revealed that the increase in State A duration was specific to responders of ECT ($t = 8.5$; $df = 12$; $p < 0.0001$; Bonferroni-corrected $p < 0.0001$; Cohen's $d = 1.60$) (middle panel of Fig. 3A). This effect was not observed in non-responders for State A ($t = 1.7$; $df = 8$; $p = 0.1$; Cohen's $d = 0.52$) (right panel of Fig. 3A). A decrease in the frequency of State B ($t = -3.1$; $df = 12$; $p = 0.008$; Bonferroni-corrected $p = 0.03$; Cohen's $d = 0.67$) (middle panel of Fig. 4B), State C ($t = -4.0$; $df = 12$; $p = 0.002$; Bonferroni-corrected $p = 0.008$; Cohen's $d = 0.90$) (middle panel of Fig. 4C) and State D ($t = -2.9$; $df = 12$; $p = 0.01$; Bonferroni-corrected $p = 0.04$; Cohen's $d = 0.71$) (middle panel of Fig. 4D) was specific to responders of ECT. This effect was not observed in non-responders for State B ($t = -0.78$; $df = 8$; $p = 0.5$; Cohen's $d = 0.24$), State C ($t = -2.0$; $df = 8$; $p = 0.08$; Cohen's $d = 0.67$) or State D ($t = -1.6$; $df = 8$; $p = 0.2$; Cohen's $d = 0.71$) (right panels of Fig. 4B–D).

3.1.3. Magnetic seizure therapy

Similar to ECT, there was an increase in duration and decrease in frequency of microstates following MST. A main effect of *Time* (F = 6.8; $df = 1,22$; $p = 0.01$; $\eta_p^2 = 0.24$) and *Microstate Class* (F = 6.4; $df = 3,66$; $p = 0.0007$; $\eta_p^2 = 0.23$) was observed in the duration feature. The interaction effect of *Time* × *Microstate Class* was not significant (F = 0.11; $df = 3,66$; $p = 0.96$; $\eta_p^2 = 0.005$). An effect of *response* was not observed (F = 2.3; $df = 1,22$; $p = 0.2$; $\eta_p^2 = 0.094$). In addition, a main effect of *Time* (F = 4.4; $df = 1,22$; $p = 0.04$; $\eta_p^2 = 0.16$) and a main effect of *Microstate Class* (F = 4.0; $df = 3,66$; $p = 0.01$; $\eta_p^2 = 0.15$) were observed in the frequency feature. The interaction effect of *Time* × *Microstate Class* was not significant (F = 0.075; $df = 3,66$; $p = 0.97$; $\eta_p^2 = 0.003$). An effect of *response* was not observed (F = 2.4; $df = 1,22$; $p = 0.1$; $\eta_p^2 = 0.10$). Apart from the main effect of *Microstate Class* (F = 5.8; $df = 3,66$; $p = 0.001$; $\eta_p^2 = 0.21$), no significant effects were observed in the coverage of microstates. See supplementary figures Fig. S5–S7. Planned comparisons were not significant (see supplementary Table 1).

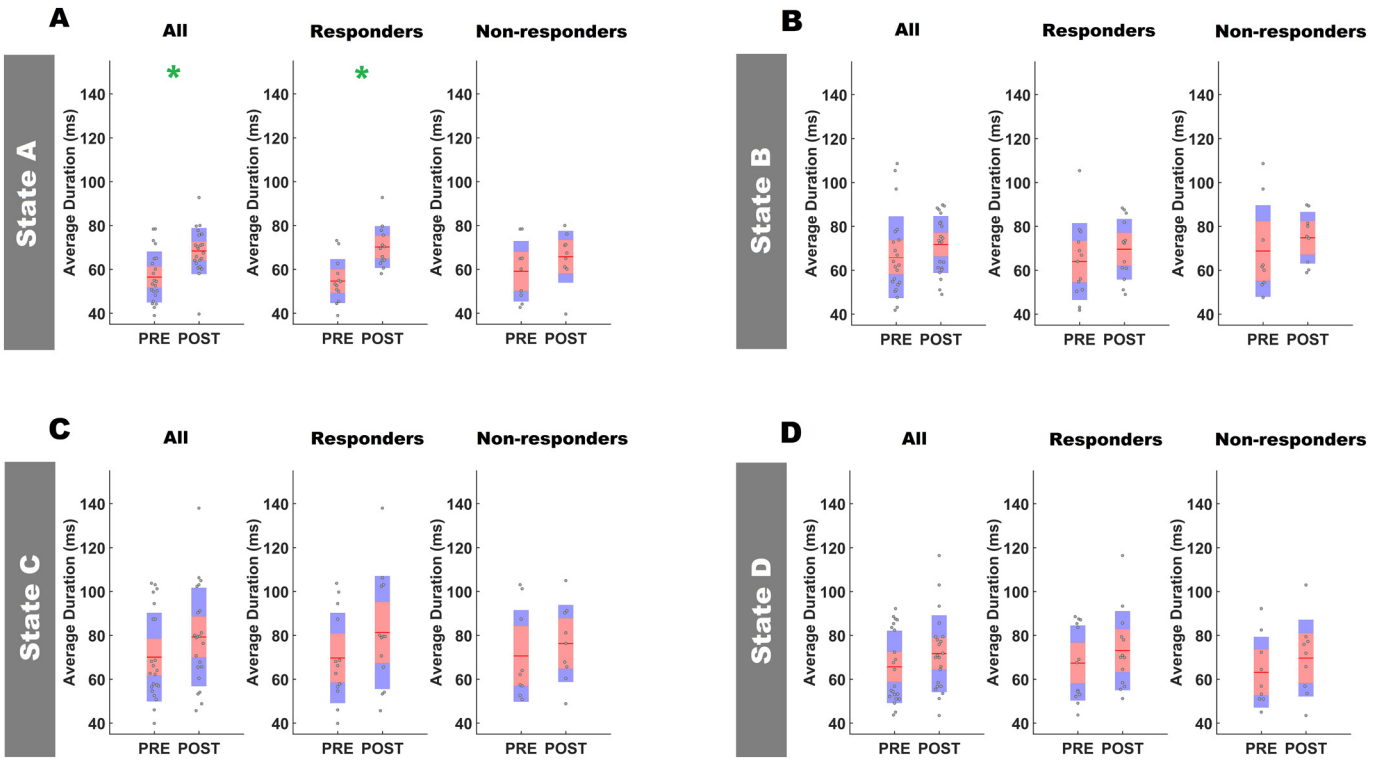

Fig. 3. Effect of electroconvulsive therapy (ECT) on the average duration of all four microstates. In each subplot, the raw data is plotted on top of a boxplot showing the mean (red line), 95% confidence interval (red area) and 1 standard deviation (blue area). Significant comparisons are marked with a green (*). **(A) Left panel:** Following ECT, there was a significant increase in the duration of State A (y-axis) ($p < 0.0001$). **Middle panel and right:** This increase was specific to responders of ECT ($p < 0.0001$). **(B)** No significant changes were observed in the duration of State B. **(C)** No significant changes were observed in the duration of State C. **(D)** No significant changes were observed in the duration of State D.

3.2. Correlation and prediction analysis results

3.2.1. Seizure therapy (ECT and MST)

An increase in the duration of State A correlated with improvement in depressive symptoms (HRSD) ($r = 0.33$, 95% CI 0.044 to 0.57, *p-corrected* = 0.02). The increase was also a fair predictor of improvement in depressive symptoms (HRSD) (AUC = 0.71, $p = 0.003$) (Fig. 5).

3.2.2. Electroconvulsive therapy

A decrease in State D duration following ECT treatment significantly correlated with improvement in self-rated depressive symptoms (BDI) ($r = -0.55$, 95% CI −0.82 to −0.09, *p-corrected* = 0.02) (left panel of Fig. 6B). The decrease was also a good predictor of improvement in self-rated depressive symptoms (BDI) (AUC = 0.83, $p = 0.0007$) (right panel of Fig. 6B). Based on the association of State C to the salience and State D to the frontoparietal network (Britz et al., 2010) and based on research indicating that the salience network facilitates the activation of the frontoparietal network (Menon and Uddin, 2010), we hypothesized that the change in State D duration relative to the change in State C duration will also significantly correlate with clinical outcome. The log ratio between change in State D duration and change in State C duration correlated with improvement in self-rated depressive symptoms (BDI) ($r = -0.67$, 95% CI −0.87 to −0.28, $p = 0.003$) (left panel of Fig. 6C) and clinical depression scores (MADRS) ($r = -0.50$, 95% CI −0.78 to −0.04, $p = 0.03$). The ratio was also an excellent predictor of improvement in self-rated depressive symptoms (BDI) (AUC = 0.97, $p < 0.0001$) (right panel of Fig. 6C).

Furthermore, an increase in State A coverage correlated with improvement in self-rated depressive symptoms (BDI) ($r = 0.57$, 95% CI 0.12 to 0.82, *p-corrected* = 0.02) (left panel of Fig. 6A). The increase was also a fair predictor of improvement in self-rated depressive symptoms (BDI) (AUC = 0.79, $p = 0.005$) (right panel of Fig. 6A).

3.2.3. Magnetic seizure therapy

Changes in microstate dynamics following MST were not associated with change in depressive symptoms (see supplementary Table 2). Baseline characteristics of all microstates were shown to predict suicidal ideation response (right panels of Fig. 7A). At baseline, a shorter duration of State A ($r = -0.57$, 95% CI −0.81 to −0.17, *p-corrected* = 0.01), State B ($r = -0.49$, 95% CI −0.77 to −0.06, *p-corrected* = 0.03), State C (r = −0.49, 95% CI −0.77 to −0.06, *p-corrected* = 0.03) and a higher frequency of State D ($r = 0.52$, 95% CI 0.10 to 0.78, *p-corrected* = 0.02) predicted suicidal ideation response. Furthermore, a decrease in State B frequency was shown to be correlated with improvement in cognition ($r = -0.50$, 95% CI −0.77 to −0.09, *p-corrected* = 0.01) (middle panel of Fig. 7B) and was a good predictor of improvement in cognition (AUC = 0.80, $p = 0.002$) (right panel of Fig. 7B).

3.3. Microstate dynamics in patients with treatment-resistant depression vs healthy controls

Patients revealed an increased duration and decreased frequency of microstates compared to healthy subjects (left panels of Fig. 8A and Fig. 8C). By comparing healthy subjects with patients before treatment, a significant main effect of *Group* (F = 4.9; *df* = 1,127; $p = 0.03$; $\eta_p^2 = 0.04$), *Microstate Class* (F = 12.2; *df* = 3,381; $p < 0.0001$; $\eta_p^2 = 0.09$) and an interaction effect of *Group* × *Microstate Class* approaching significance (F = 2.1; *df* = 3,381; $p = 0.09$; $\eta_p^2 = 0.02$) was observed in the duration of microstates. A main effect of *Group* (F = 4.4; *df* = 1,127; $p = 0.03$; $\eta_p^2 = 0.03$), *Microstate Class* (F = 7.6; *df* = 3,381; $p = 0.01$; $\eta_p^2 = 0.06$) and an interaction effect of *Group* × *Microstate Class* (F = 3.8; *df* = 3,381; $p = 0.01$; $\eta_p^2 = 0.03$) was

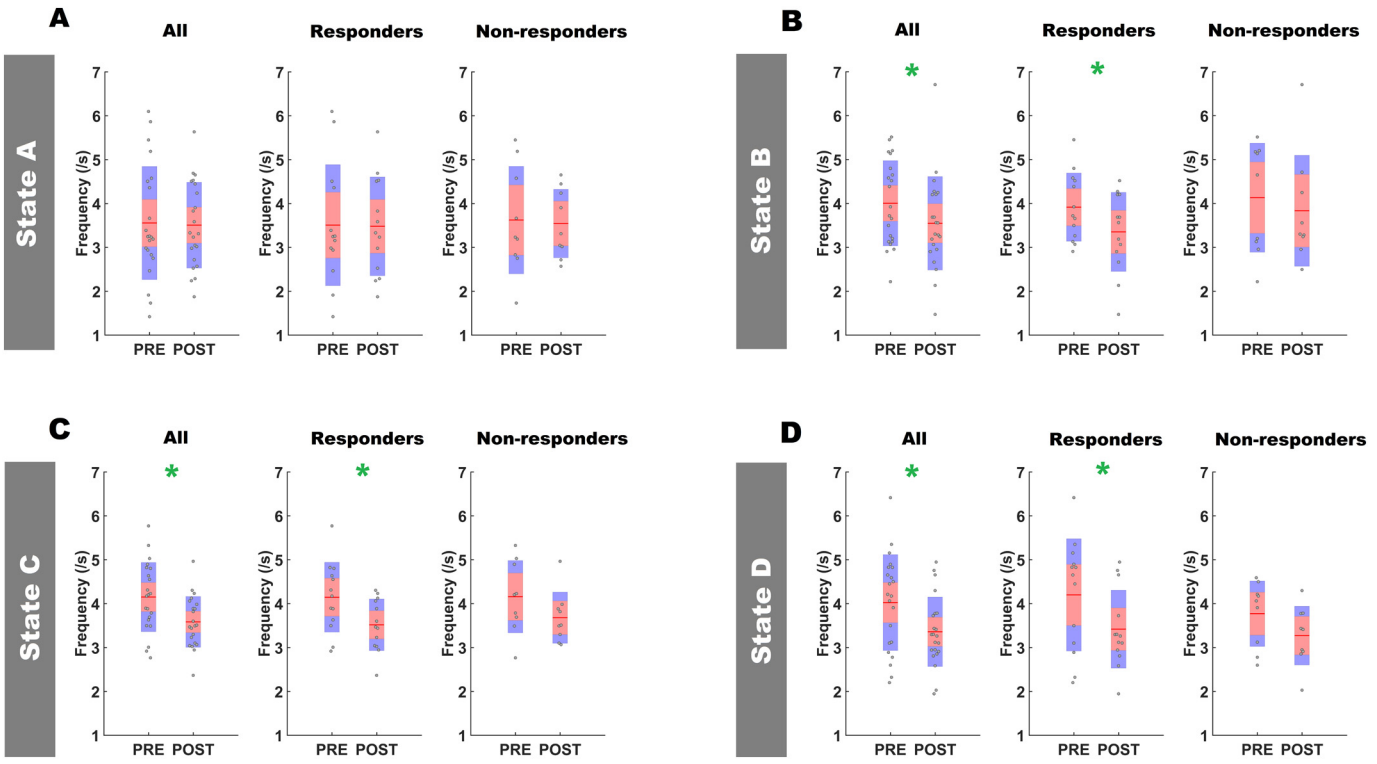

Fig. 4. Effect of electroconvulsive therapy (ECT) on the frequency of all four microstates. In each subplot, the raw data is plotted on top of a boxplot showing the mean (red line), 95% confidence interval (red area) and 1 standard deviation (blue area). Significant comparisons are marked with a green (*). **(A)** No significant changes were observed in the frequency of State A. **(B) Left panel:** A decrease in the frequency of State B (y-axis) was observed following ECT ($p = 0.03$). **Middle and right panels:** This decrease in frequency of State B was specific to responders of ECT ($p = 0.03$). **(C) Left panel:** A decrease in the frequency of State C (y-axis) was observed following ECT ($p = 0.002$). **Middle and right panels:** This decrease in frequency of State C was specific to responders of ECT ($p = 0.008$). **(D) Left panel:** A decrease in the frequency of State D (y-axis) was observed following ECT ($p = 0.0003$). **Middle and right panels:** This decrease in frequency of State D was specific to responders of ECT ($p = 0.04$).

observed in the frequency of microstates.

A significant main effect of *Microstate Class* (F = 1.0; *df* = 3,381; $p < 0.0001$; $\eta_p^2 = 0.08$) and a significant interaction of *Group* × *Microstate Class* (F = 3.5; *df* = 3,381; $p = 0.01$; $\eta_p^2 = 0.03$) was observed with the coverage feature between healthy subjects and patients at baseline (Fig. 8E). The main effect of *Group* was not significant (F = 2.1; *df* = 1,127; $p = 0.2$; $\eta_p^2 = 0.02$).

3.4. Microstate dynamics in patients with treatment-resistant depression following seizure therapy vs healthy controls

The longer duration and lower frequency of microstates in patients persisted following treatment (Fig. 8B and D). Comparing healthy subjects with patients after seizure therapy, there was a main effect of *Group* (F = 19.4; *df* = 1,98; $p < 0.0001$; $\eta_p^2 = 0.17$) and *Microstate Class* (F = 12.1; *df* = 3,294; $p < 0.0001$; $\eta_p^2 = 0.11$) in the duration feature. The interaction of *Group* × *Microstate Class* was not significant (F = 1.1; *df* = 3,294; $p = 0.36$; $\eta_p^2 = 0.01$). In the frequency feature,

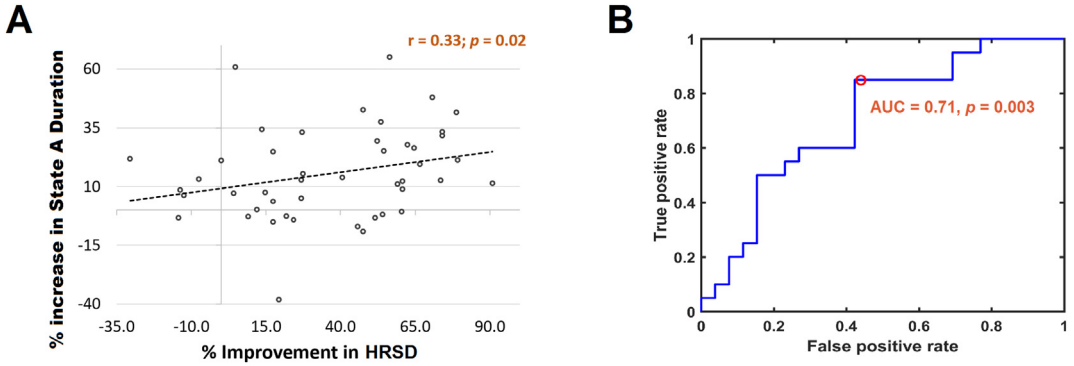

Fig. 5. Change in the duration of State A following seizure therapy (ECT + MST) correlated with improvement in depressive symptoms (HRSD). For the receiver operating characteristic (ROC) curve (right panels), the x-axes represents the false positive rate (1-specificity) and the y-axes represents the true positive rate (sensitivity). The red circle depicts the optimum operating point of the ROC curve. The area under the curve (AUC) at this optimum point is specified on the graph. **(A)** An increase in the duration of State A significantly correlated with improvement in depressive symptoms (x-axis), Hamilton Rating Scale for Depression (HRSD) (r = 0.33, $p = 0.02$). X-axis represents change in HRSD (pre-post)/(pre*100). Y-axis represents change in coverage of State D (post-pre)/(pre*100). **(B)** Change in State A duration was also a fair predictor of response to seizure therapy (AUC = 0.71, $p = 0.003$).

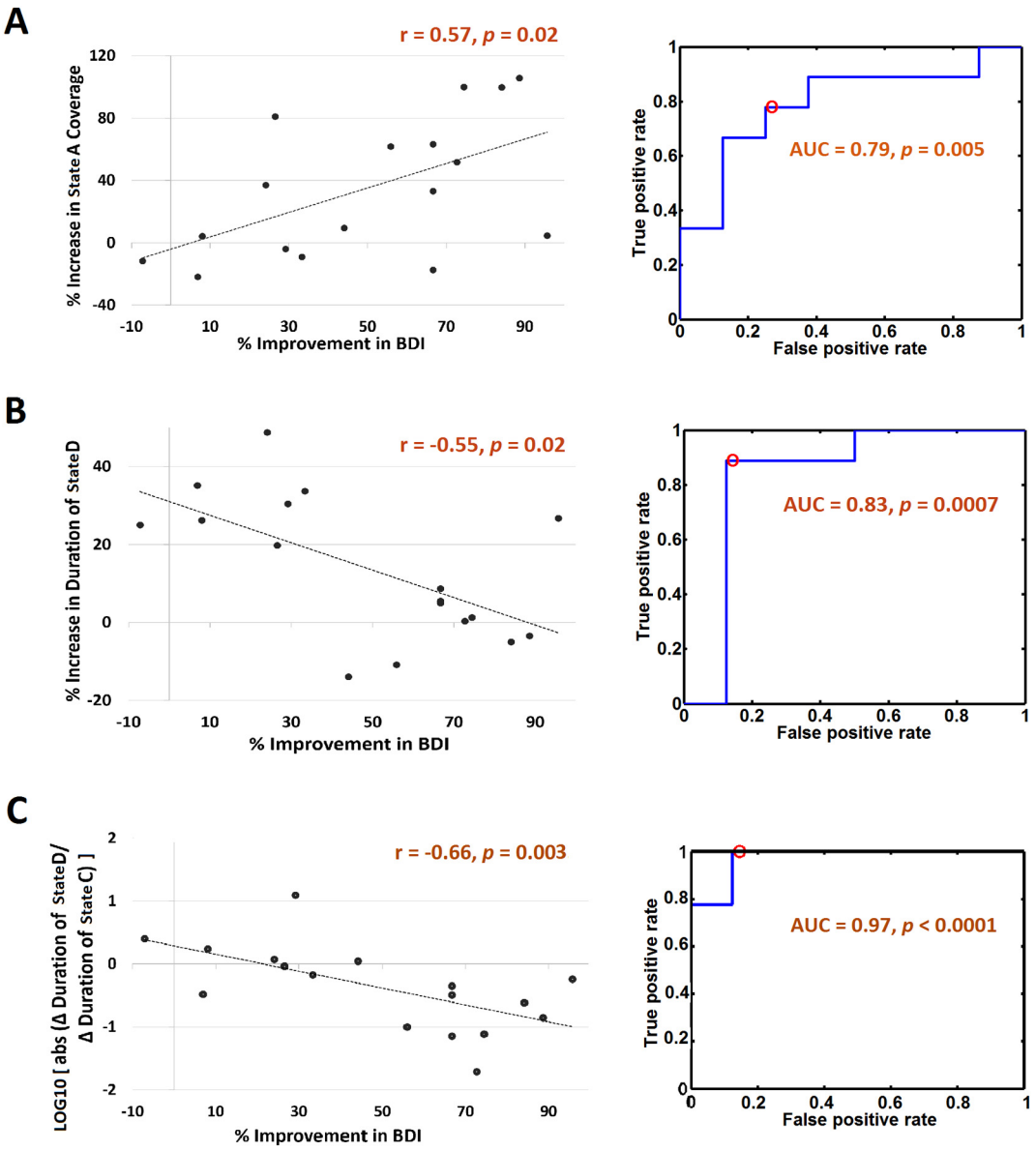

Fig. 6. Changes in microstate characteristics following electroconvulsive therapy (ECT) correlated with improvement in self-rated depressive symptoms. For the receiver operating characteristic (ROC) curves (all right panels), the x-axes represents the false positive rate (1-specificity) and the y-axes represents the true positive rate (sensitivity). The red circle depicts the optimum operating point of the ROC curve. The area under the curve (AUC) at this optimum point is specified on the graph. **(A) Left panel:** An increase in the coverage of State A significantly correlated with improvement in self-rated depressive symptoms (x-axis), Beck's Depression Inventory scale (BDI) (r = 0.57, p = 0.02). X-axis represents change in BDI (pre-post)/(pre*100). Y-axis represents change in coverage of State D (post-pre)/(pre*100). **Right panel:** Change in State A coverage was also a strong predictor of response to ECT (BDI) (AUC = 0.79, p = 0.005). **(B) Left panel:** A decrease in the duration of State D was significantly correlated with improvement in BDI ($r = -0.55$, p = 0.02). X-axis represents change in BDI (pre-post)/(pre*100). Y-axis represents change in duration of State D (post-pre)/(pre*100). **Right panel:** Change in State D duration was also a strong predictor of response to ECT (BDI) (AUC = 0.83, p = 0.0007). **(C) Left panel:** The correlation between State D duration and BDI remained significant when the change in duration of State D was presented relative to the change in duration of State C ($r = -0.66$, p = 0.003). X-axis represents change in BDI (pre-post)/(pre*100). Y-axis represents the log of the absolute ratio between change in duration of State D (post-pre)/(pre*100) over the change in duration of State C (post-pre)/(pre*100). **Right panel:** Ratio of change in State D duration over the change in State C duration was an excellent predictor of self-rated response to ECT (BDI) (AUC = 0.97, $p < 0.0001$).

there was a significant main effect of *Group* (F = 16.3; *df* = 1,98; p = 0.0001; η_p^2 = 0.14) and *Microstate Class* (F = 6.1; *df* = 3,294; p = 0.0005; η_p^2 = 0.06). The interaction of *Group* × *Microstate Class* was not significant (F = 1.5; *df* = 3,294; p = 0.22; η_p^2 = 0.02).

The main effect of *Microstate Class* was significant in the coverage feature (F = 8.8; *df* = 3,294; $p < 0.0001$; η_p^2 = 0.08). The main effect of Group (F = 1.4; *df* = 1,98; p = 0.24; η_p^2 = 0.003) and the interaction effect of *Group* × *Microstate Class* (F = 1.2; *df* = 3,294; p = 0.32; η_p^2 = 0.01) were not significant (Fig. 8E).

3.5. Source localization of the global-clustered microstates

In Fig. 9, the global-clustered microstates are shown alongside their corresponding eLORETA images. All states show a common neural generator in the posterior cingulate and cingulate gyrus. This has been shown in previous literature (Pascual-Marqui et al., 2014). State A was associated with the left superior and middle temporal gyrus (Fig. 9A). State B with the cuneus and precuneus of the occipital lobe (Fig. 9B). State C was best associated with the anterior cingulate, insula and cuneus and precuneus of the occipital lobe (Fig. 9C). Finally, State D with

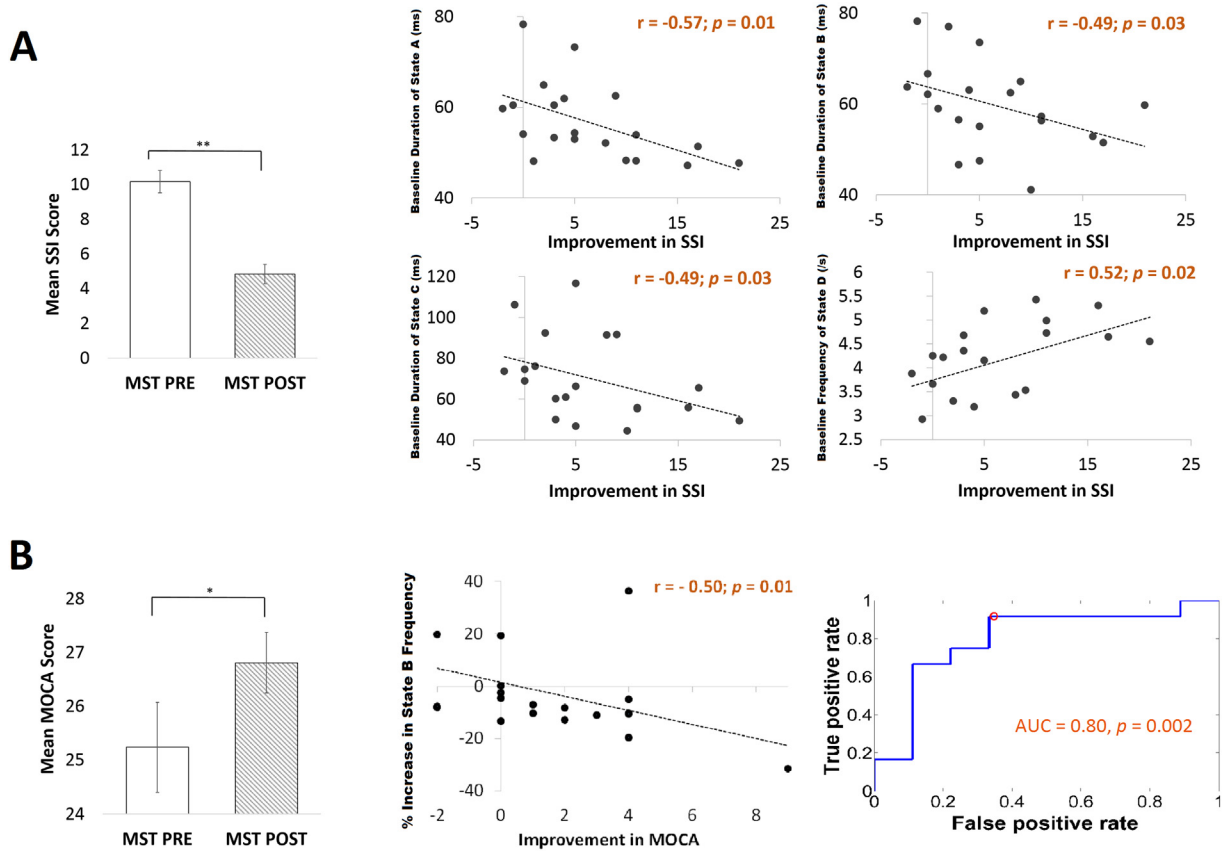

Fig. 7. Effect of magnetic seizure therapy (MST) on microstate characteristics. (A) Left panel: Following MST, patients showed a significant improvement in scale for suicidal ideation (SSI). **Middle and right panels:** Reduction in SSI was significantly associated with baseline resting-state microstate characteristics of all microstate classes. X-axes represents change in SSI score (Post-Pre) and y-axes represents baseline characteristics of each microstate A, B, C and D. **(B) Left panel:** Following MST, patients showed a significant improvement in cognition scores (Montreal Cognitive Assessment (MOCA)). **Middle panel:** A decrease in the frequency of State B following MST correlated with improvement in cognition scores. X-axis represents change in MOCA (Post-Pre) and y-axis represent change in State B frequency (post-pre)/(pre*100). **Right panel:** This decrease in frequency was also a strong predictor of cognitive score outcome. The x-axis represents the false positive rate (1-specificity) and the y-axis represents the true positive rate (sensitivity). The red circle depicts the optimum operating point of the receiver operating characteristic curve. The area under curve (AUC) at this optimum point is specified on the graph (AUC = 0.80, p = 0.002).

the paracentral lobe of the frontal lobe, the precuneus of the parietal lobe, the parahippocampal gyrus of the limbic lobe, and the lingual gyrus of the occipital lobe (Fig. 9D). See Fig. S8-S11 for more detailed images of source localization.

3.6. Power spectral density analysis

3.6.1. Neuronal oscillations in patients vs healthy controls

No significant differences were observed in relative power between the healthy and patient groups after cluster-based permutation correction for multiple comparisons (Fig. S12).

3.6.2. Effect of seizure therapy on neuronal oscillations

Following cluster-based permutation correction, both ECT responders and non-responders revealed an increase in relative power of slow cortical oscillations (1–7 Hz) and a decrease in relative power of oscillations above 10 Hz (Fig. S13A–B). The increase in relative power of slow cortical oscillations was not observed in responders or non-responders of MST (Fig. S13C–D). Common to ECT and MST however, was a decrease in relative power above 17 Hz. In responders of MST, a decrease in relative power was observed above 17 Hz. In non-responders of MST, a decrease in relative power was observed above 11 Hz.

3.6.3. Microstate dynamics and neuronal oscillations

In the ECT group, the increase in slow oscillations was not correlated with microstate characteristics (Fig. S14). Only changes in the low beta and high beta power bands correlated with change in duration and frequency of microstates. A significant change in duration of microstates following ECT was specific to State A. However, changes in low beta and high beta were correlated with changes in duration of States B and C. Significant change in frequency of microstates following ECT was specific to States B, C and D. Yet, change in low beta correlated with change in frequency of States A and D and change in high beta correlated with change in frequency of States A, B and D. In the MST group, none of the power bands significantly correlated with microstate characteristics (Fig. S15).

4. Discussion

This study presents the first evidence for the modulation of resting-state EEG microstate dynamics by seizure therapy in patients with treatment-resistant depression. First, several changes in microstate dynamics following seizure therapy suggested that ECT selectively modifies global brain network dynamics. An increase in the duration of State A and a decrease in the frequency of States B, C and D were associated with response to seizure therapy (specifically ECT). Although there was a change in network dynamics following MST, it was not network-specific and it was not specific to responders. However, a decrease in the frequency of State B was associated with improvement in cognition following MST. In addition, baseline microstate dynamics were shown to predict suicidal ideation response to MST (shorter

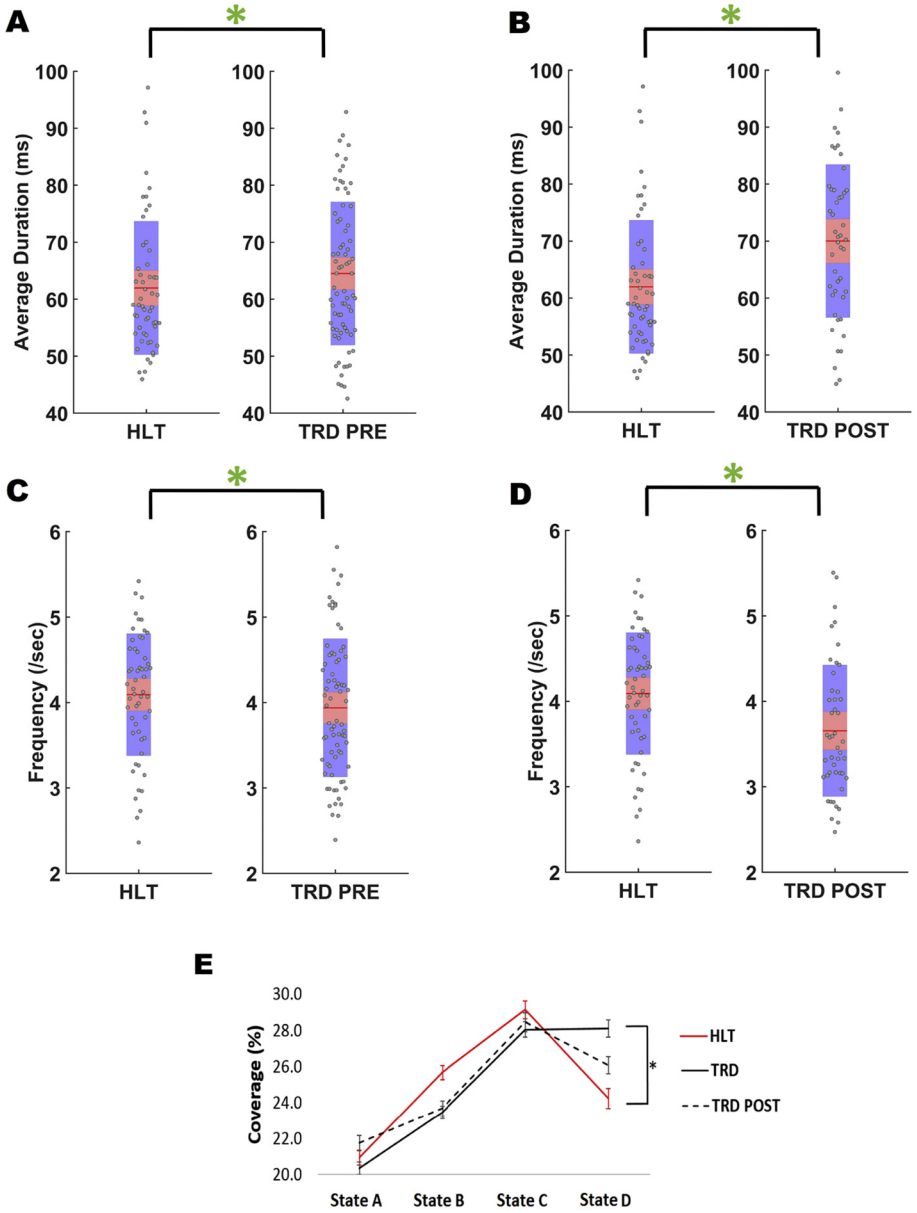

Fig. 8. Microstate characteristics of treatment-resistant depression (TRD) compared to healthy (HLT) subjects before and after seizure therapy. In each subplot, the raw data is plotted on top of a boxplot showing the mean (red line), 95% confidence interval (red area) and 1 standard deviation (blue area). All comparisons shown in **(A)** to **(D)** were significant. **(A) & (B)** Patients showed a longer duration ($p = 0.03$) and lower frequency ($p = 0.03$) of microstate dynamics compared to healthy subjects. **(C) & (D)** Following seizure therapy, patients showed a much longer duration ($p < 0.0001$) and lower frequency ($p = 0.0001$) of microstates compared to healthy subjects. In all plots of (**A–D**, x-axes represents the subject group. In **(A–B)**, y-axis represents the duration of all microstates in milliseconds (main effect of group in ANCOVA). In **(C–D)**, y-axis represents the frequency of all microstates per second (main effect of group in ANCOVA). **(E)** Seizure therapy (ECT and MST) was shown to normalize the high coverage of State D in patients compared to healthy subjects ($p = 0.01$). X-axis represents each microstate class. Y-axis represents the percent coverage of all microstates, and each line in the graph represents a subject group (interaction effect of M*icrostate Class* × *Group* in ANCOVA).

duration of States A, B, C and a higher frequency of State D). Finally, patients revealed increased duration and decreased frequency of microstates compared to healthy subjects. Following seizure therapy, this difference was greater between patients and healthy subjects. Collectively, these findings provide insight into the role of global network dynamics in the potential mechanism of action of seizure therapy for treatment-resistant depression.

Although the most effective treatment for treatment-resistant depression is ECT, its underlying mechanism of action is not clearly understood. In this study, a significant increase in the duration of State A and decrease in the frequency of States B, C and D was observed in responders of seizure therapy (specifically ECT). We hypothesize that this might reflect a relative stabilization (or reduction) of microstate dynamics since it infers that the microstate occurs for a longer duration of time and is less variable (i.e., more stable). This finding may support one of the main theories on the efficacy of ECT, the anticonvulsant hypothesis (Coffey et al., 1995; Sackeim, 1999). The anticonvulsant hypothesis suggests that an activation of inhibitory mechanisms initially occurs to inhibit seizures caused by ECT but eventually leads to the inhibition of hyperactive networks in depression, which may lead to reduced global network dynamics. There is a large amount of accumulating evidence for the anticonvulsant hypothesis, such as increased cortical GABA (Sanacora et al., 2003), decreased regional brain metabolism (Hoy et al., 2013), increased slow-wave EEG activity as well as decreased seizure duration and increased seizure threshold over the course of ECT (Sackeim, 1999). The potential stabilization of microstate (i.e., global network) dynamics following seizure therapy further adds to this line of evidence.

In a recent comprehensive meta-analysis of resting-state fMRI studies (Kaiser et al., 2015), depression was associated with aberrant interactions between the salience, frontoparietal and default-mode networks, argued to be the facilitators of depressive symptoms. With recent progress in the integration of fMRI and EEG data, a few studies have explored the association between cortical microstate activity and resting-state fMRI networks (Musso et al., 2010; Schwab et al., 2015; Jann et al., 2010). In *Britz* et al. *(Britz et al., 2010)*, the salience and frontoparietal networks were associated with States C and D. As hypothesized in this study, the frequency of States C and D decreased following seizure therapy and these changes were associated with treatment response (specifically ECT). In addition, change in State D

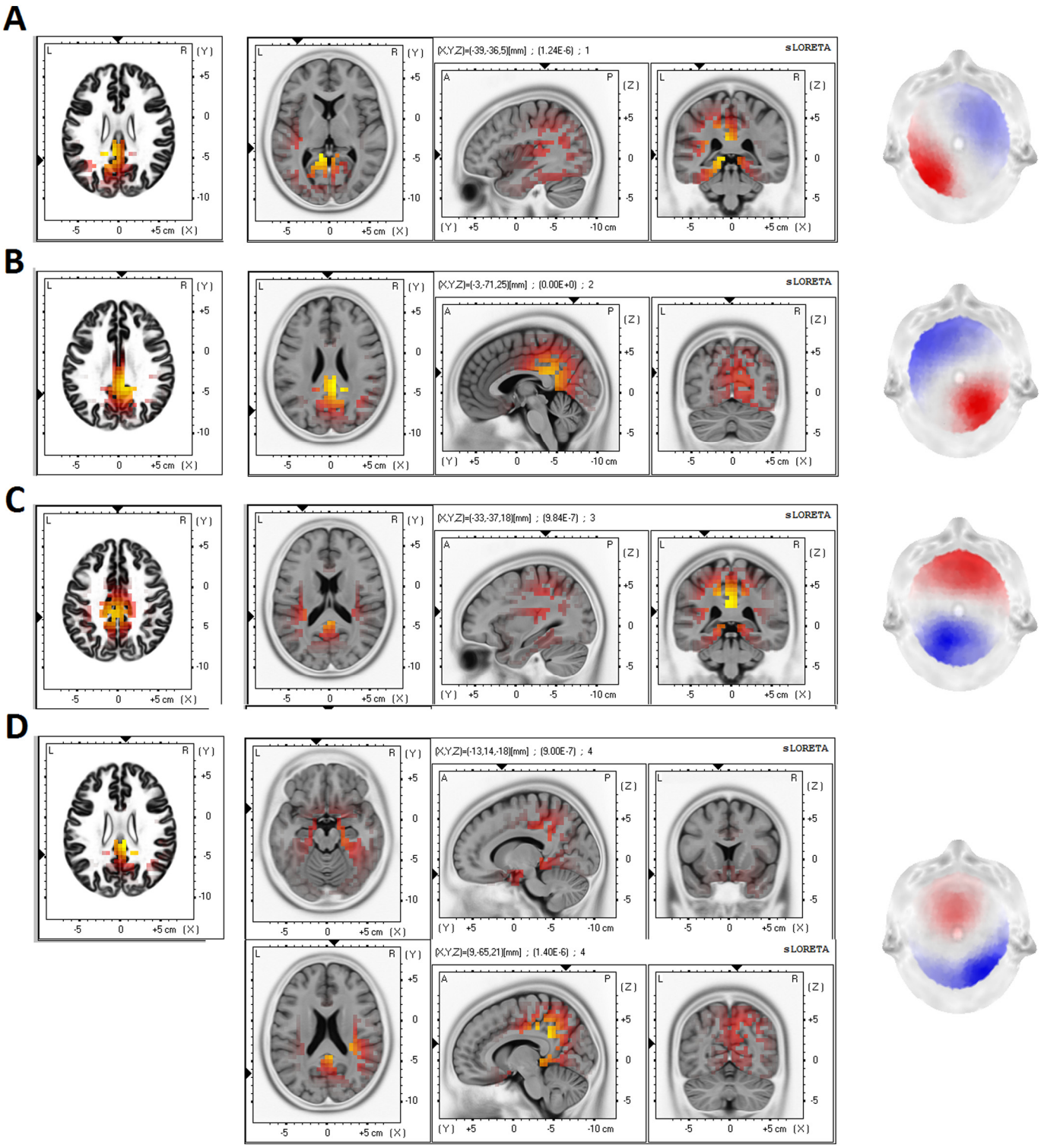

Fig. 9. Global microstate classes clustered over all groups and all subjects with their source (eLORETA) images. All microstates show activation in the posterior cingulate gyrus. **(A)** Microstate A was shown to be associated with the left superior and middle temporal gyrus. **(B)** Microstate B was associated with the cuneus and precuneus of the occipital lobe. **(C)** Microstate C was associated with the anterior cingulate, insula and cuneus and precuneus of the occipital lobe. **(D)** Microstate D was associated with the paracentral lobe of the frontal lobe, the precuneus of the parietal lobe, the parahippocampal gyrus, and the lingual gyrus of the occipital lobe.

duration relative to the change in State C duration correlated with improvement in depressive symptoms following ECT. This suggests that the interaction between the neural generators underlying these microstates may be impaired in patients with treatment-resistant depression, and may be linked to the role of State C as a dynamic "switching network". This role of State C has been widely postulated in schizophrenia-related microstate research (Rieger et al., 2016).

As an alternate to ECT, MST was proposed to minimize cognitive side effects while maintaining antidepressant efficacy. A few studies have even associated MST with improvement in cognition including

visual-spatial learning, memory and phonological tasks (Lisanby et al., 2003; Kayser et al., 2011; Kayser et al., 2015). The association between change in State B frequency and improvement in cognition with MST may be in line with these findings since State B has been associated with the parietal and occipital-parietal areas of spatial-visualization and verbalization (Britz et al., 2010; Milz et al., 2016b). In addition to cognition, MST was previously associated with remission of suicidal ideation. Baseline markers of inhibitory neurotransmission were shown to predict therapeutic efficacy of MST in reducing suicidal ideation (Sun et al., 2016). In our study, baseline microstate dynamics (of all four states) predicted the therapeutic efficacy of MST in reducing suicidal ideation. Source localization revealed that all four microstates had in common the posterior cingulate cortex and the precuneus, regions linked with the default-mode network. This suggests that MST may be able to target the impaired default-mode network in treatment-resistant depression (Kaiser et al., 2015). The coil position of MST in this study supports this hypothesis as the greatest induced electrical field was over one of the hubs of the default-mode network, the dorsomedial prefrontal cortex. We suggest that MST modulates neural networks impaired in treatment-resistant depression but may not be as robust as ECT due to the sub-optimal induced electric field potentials.

As mentioned, patients that have previously received two or more courses of antidepressants with no clinical outcome are treatment-resistant. Detailed fMRI studies between healthy subjects and patients with and without treatment-resistant depression have indicated that different functional connectivity patterns may be associated with treatment-resistance (Yamamura et al., 2016; Wu et al., 2011; Guo et al., 2011), potentially due to the previous antidepressant exposure in treatment-resistant depression. Several neuroimaging studies have shown that treatment can change resting-state brain dynamics regardless of clinical outcome (Fu et al., 2013; Mayberg et al., 1997; Mayberg, 2003; Kennedy et al., 2001). In this study, a longer duration and lower frequency of microstates were observed in patients with treatment-resistant depression compared to healthy subjects. We link this effect to the neurotropic medications previously taken by these patients. Although the patients in this study did not respond to their previous treatments, we hypothesize that each treatment they received may have had an effect on global brain dynamics. It has been shown that benzodiazepines and antipsychotics can modulate microstate dynamics (Kinoshita et al., 1995). Following seizure therapy, a larger increase in duration and decrease in frequency of microstates was observed in our study, suggesting that antidepressants and seizure therapy may modulate global brain dynamics in a similar manner. Considering the association of these changes to therapeutic outcome in seizure therapy, we hypothesize that seizure therapy overcomes the inadequacy of medications in treatment-resistant depression through a stronger impact on network dynamics. However, in the absence of a control group, i.e., patients without treatment-resistant depression and longitudinal assessments, it remains to be investigated whether this is an effect of treatment-resistance, medication, or both.

The higher efficacy of seizure therapy in treatment-resistant depression has been linked with the stimulation of thalamic oscillatory pacemakers and re-setting of neural dynamics (Farzan et al., 2014). Studies have also highlighted the importance of temporal variability in affective and cognitive brain functions (Stam et al., 2006; Rubinov and Sporns, 2010; Tononi et al., 1994). A recent study showed a link between timescale-dependent and region-specific modulation of temporal complexity and the affective and cognitive impacts of seizure therapy (Farzan et al., 2017). For example, association between change in complexity and improvement in depressive symptoms was localized to the fronto-central and parieto-occipital regions (Farzan et al., 2017). In the current study, by observing the temporal stability of brain network dynamics rather than temporal complexity, we provide complimentary evidence suggesting that the therapeutic impact of seizure therapy is network-specific. States C and D were consistently associated with response to seizure therapy and these states were in part localized to the frontal, parietal and occipital regions.

There is strong evidence suggesting that seizure therapy impacts neuronal oscillations. Traditional power spectral density analysis has shown that the slowing of EEG oscillations following ECT is associated with improvement in depressive symptoms (Sackeim et al., 1996). Power spectral density analysis in our study also revealed increased slow wave activity following ECT. However, this effect was observed in both responders and non-responders. In comparison, microstate analysis illustrated that ECT responders show significant changes in certain microstates (A in duration and B, C, & D in frequency) while non-responders do not. In addition, changes in microstate dynamics were not associated with the increase in power of slow oscillations. Microstate analysis also demonstrated that patients with treatment-resistant depression reveal different global brain dynamics compared to healthy subjects and also that microstate D may play an important role in this difference. While we identified differences in microstate characteristics, no significant differences were observed in power between patients with treatment-resistant depression and healthy subjects. These findings suggest that microstate analysis provide additional and perhaps independent information compared to power spectral density analysis.

There are some limitations to this study. First, treatment-resistant depression may be too broad and heterogeneous to be treated in a homogenous manner. Although patients are grouped together under the definition of treatment-resistant depression (i.e., failed to respond to two or more antidepressants), as seen in this study, they still show heterogeneity in their response to treatments such as seizure therapy. This suggests that there is still considerable heterogeneity in the population of treatment-resistant depression which can translate to variability in the derived neurophysiological markers such as microstate characteristics. Results of this study will therefore need validation with a larger sample size. In addition, due to the small sample size, treatment parameters such as stimulation location (bilateral or unilateral for ECT) and frequency (for MST) could not be controlled. The potential effects these parameters may have on microstate characteristics need to be explored and validated by larger samples in future work. Preregistration of such future studies in advance of data collection and analysis is encouraged.

5. Conclusions

The present study provides insight into the mechanism of action of successful seizure therapy for treatment-resistant depression using resting-state EEG microstate analysis. First, an increased duration and decreased frequency of microstates was observed in responders of seizure therapy, specifically ECT. This provides complementary evidence to recent neuroimaging studies which suggest that seizure therapy may stabilize global network dynamics in treatment-resistant depression. In MST, this modulation was a trend-level effect, implying that ECT may have a stronger impact on global neural networks than MST. Second, baseline microstate dynamics were indicative of MST-related improvement in cognition and suicidal ideation. Third, contrary to our hypothesis, we showed reduced global network dynamics in treatment-resistant depression when compared with healthy subjects. We hypothesized that this may be caused by previous antidepressants taken by these patients. Seizure therapy was shown to further reduce these dynamics and this reduction was associated with clinical response. This suggests that antidepressant medications and seizure therapy may have an analogous effect on network dynamics. However, only the modulation of global network dynamics by seizure therapy may be associated with clinical response. Finally, state-specific changes in microstate dynamics were observed in responders of seizure therapy. Microstates previously linked to resting-state networks known to be disrupted in depression (C and D), were associated with seizure therapy response. Further work is required to evaluate microstates as a therapeutic target in developing novel antidepressant treatments.

Financial disclosures

SA, WW, SM, and FF have no financial disclosures to report. DMB receives non-salary operating funds and in-kind equipment support from Brainsway Ltd. for an investigator-initiated study. He is the site principal investigator for several sponsor-initiated clinical trials from Brainsway Ltd. He receives in-kind equipment support from Tonika/Magventure for an investigator-initiated study. In the last 3 years, ZJD has received research and equipment in-kind support for an investigator-initiated study through Brainsway Inc. and Magventure Inc.

Acknowledgements

This work is supported in part by the Ontario Graduate Scholarship and the Walter C. Sumner Memorial Fellowship awarded to SA. FF received research support from the Natural Sciences and Engineering Research Council of Canada (NSERC), and Brain and Behavior Research Foundation (formerly NARSAD). DMB receives research support from the Canadian Institutes of Health Research (CIHR), Brain Canada, National Institutes of Health (NIH), Temerty Family through the Centre for Addiction and Mental Health (CAMH) Foundation and the Campbell Family Research Institute. ZJD was supported by the Ontario Mental Health Foundation (OMHF), the Canadian Institutes of Health Research (CIHR), the Brain and Behaviour Research Foundation and the Temerty Family and Grant Family through the Centre for Addiction and Mental Health (CAMH) Foundation and the Campbell Institute. Funding sources had no role in the design, collection, analysis and interpretation of the study. Finally, this study would not be possible without the numerous volunteers. We would also like to acknowledge the research and medical staff at the Temerty Centre for Therapeutic Brain Stimulation for their support, assistance and dedication.

Appendix A. Supplementary data

Supplementary data to this article can be found online at https://doi.org/10.1016/j.nicl.2018.10.015.

References

Abbott, C.C., Gallegos, P., Rediske, N., Lemke, N.T., Quinn, D.K., 2014. A review of longitudinal electroconvulsive therapy: neuroimaging investigations. J. Geriatr. Psychiatry Neurol. 27, 33–46.
Bassett, D.S., Bullmore, E., 2006. Small-world brain networks. Neuroscientist 12, 512–523.
Berlim, M.T., Turecki, G., 2007. Definition, assessment, and staging of treatment—resistant refractory major depression: a review of current concepts and methods. Can. J. Psychiatr. 52, 46–54.
Brandeis, D., Naylor, H., Halliday, R., Callaway, E., Yano, L., 1992. Scopolamine effects on visual information processing, attention, and event-related potential map latencies. Psychophysiology 29, 315–335.
Britz, J., Van De Ville, D., Michel, C.M., 2010. BOLD correlates of EEG topography reveal rapid resting-state network dynamics. NeuroImage 52, 1162–1170.
Brodbeck, V., Kuhn, A., von Wegner, F., Morzelewski, A., Tagliazucchi, E., Borisov, S., et al., 2012. EEG microstates of wakefulness and NREM sleep. NeuroImage 62, 2129–2139.
Brunet, D., Murray, M.M., Michel, C.M., 2011. Spatiotemporal analysis of multichannel EEG: CARTOOL. Comput. Intell. Neurosci. 2011, 2.
Buckner, R.L., Sepulcre, J., Talukdar, T., Krienen, F.M., Liu, H., Hedden, T., et al., 2009. Cortical hubs revealed by intrinsic functional connectivity: mapping, assessment of stability, and relation to Alzheimer's disease. J. Neurosci. 29, 1860–1873.
Chang, C., Glover, G.H., 2010. Time–frequency dynamics of resting-state brain connectivity measured with fMRI. NeuroImage 50, 81–98.
Coffey, C.E., Lucke, J., Weiner, R.D., Krystal, A.D., Aque, M., 1995. Seizure threshold in electroconvulsive therapy (ECT) II. The anticonvulsant effect of ECT. Biol. Psychiatry 37, 777–788.
Cretaz, E., Brunoni, A.R., Lafer, B., 2015. Magnetic seizure therapy for unipolar and bipolar depression: a systematic review. Neural Plast. 2015.
de Kwaasteniet, B.P., Rive, M.M., Ruhé, H.G., Schene, A.H., Veltman, D.J., Fellinger, L., et al., 2015. Decreased resting-state connectivity between neurocognitive networks in treatment resistant depression. Front. Psychiatr. 6.
Delorme, A., Makeig, S., 2004. EEGLAB: an open source toolbox for analysis of single-trial EEG dynamics including independent component analysis. J. Neurosci. Methods 134, 9–21.
Deng, Z.-D., Lisanby, S.H., Peterchev, A.V., 2011. Electric field strength and focality in electroconvulsive therapy and magnetic seizure therapy: a finite element simulation study. J. Neural Eng. 8, 016007.
Deng, Z.-D., Lisanby, S.H., Peterchev, A.V., 2013. Controlling stimulation strength and focality in electroconvulsive therapy via current amplitude and electrode size and spacing: comparison with magnetic seizure therapy. J. ECT 29, 325.
Deng, Z.-D., McClintock, S.M., Oey, N.E., Luber, B., Lisanby, S.H., 2015. Neuromodulation for mood and memory: from the engineering bench to the patient bedside. Curr. Opin. Neurobiol. 30, 38–43.
Devanand, D., Sobin, C., Sackeim, H., 1995. Predictors of retrograde amnesia following ECT. Am. J. Psychiatry 152, 995–1001.
Farzan, F., Boutros, N.N., Blumberger, D.M., Daskalakis, Z.J., 2014. What does the electroencephalogram tell us about the mechanisms of action of ECT in major depressive disorders? J. ECT 30, 98–106.
Farzan, F., Atluri, S., Mei, Y., Moreno, S., Levinson, A.J., Blumberger, D.M., et al., 2017. Brain temporal complexity in explaining the therapeutic and cognitive effects of seizure therapy. Brain J. Neurol. 140, 1011–1025.
Fava, M., 2003. Diagnosis and definition of treatment-resistant depression. Biol. Psychiatry 53, 649–659.
Fekadu, A., Wooderson, S.C., Markopoulo, K., Donaldson, C., Papadopoulos, A., Cleare, A.J., 2009. What happens to patients with treatment-resistant depression? A systematic review of medium to long term outcome studies. J. Affect. Disord. 116, 4–11.
Fischer, A.S., Keller, C.J., Etkin, A., 2016. The clinical applicability of functional connectivity in depression: Pathways toward more targeted intervention. Biol. Psychiatry 1, 262–270.
Fox, M.D., Buckner, R.L., Liu, H., Chakravarty, M.M., Lozano, A.M., Pascual-Leone, A., 2014. Resting-state networks link invasive and noninvasive brain stimulation across diverse psychiatric and neurological diseases. Proc. Natl. Acad. Sci. 111, E4367–E4375.
Fu, C.H., Steiner, H., Costafreda, S.G., 2013. Predictive neural biomarkers of clinical response in depression: a meta-analysis of functional and structural neuroimaging studies of pharmacological and psychological therapies. Neurobiol. Dis. 52, 75–83.
Garrity, A.G., Pearlson, G.D., McKiernan, K., Lloyd, D., Kiehl, K.A., Calhoun, V.D., 2007. Aberrant "default mode" functional connectivity in schizophrenia. Am. J. Psychiatr. 164, 450–457.
Greicius, M., 2008. Resting-state functional connectivity in neuropsychiatric disorders. Curr. Opin. Neurol. 21, 424–430.
Greicius, M.D., Flores, B.H., Menon, V., Glover, G.H., Solvason, H.B., Kenna, H., et al., 2007. Resting-state functional connectivity in major depression: abnormally increased contributions from subgenual cingulate cortex and thalamus. Biol. Psychiatry 62, 429–437.
Hamilton, J.P., Furman, D.J., Chang, C., Thomason, M.E., Dennis, E., Gotlib, I.H., 2011. Default-mode and task-positive network activity in major depressive disorder: implications for adaptive and maladaptive rumination. Biol. Psychiatry 70, 327–333.
Heijnen, W.T., Birkenhäger, T.K., Wierdsma, A.I., van den Broek, W.W., 2010. Antidepressant pharmacotherapy failure and response to subsequent electroconvulsive therapy: a meta-analysis. J. Clin. Psychopharmacol. 30, 616–619.
Honey, C.J., Kötter, R., Breakspear, M., Sporns, O., 2007. Network structure of cerebral cortex shapes functional connectivity on multiple time scales. Proc. Natl. Acad. Sci. 104, 10240–10245.
Hoy, K.E., Thomson, R.H., Cherk, M., Yap, K.S., Daskalakis, Z.J., Fitzgerald, P.B., 2013. Effect of magnetic seizure therapy on regional brain glucose metabolism in major depression. Psychiatry Res. Neuroimaging 211, 169–175.
Hutchison, R.M., Womelsdorf, T., Allen, E.A., Bandettini, P.A., Calhoun, V.D., Corbetta, M., et al., 2013. Dynamic functional connectivity: promise, issues, and interpretations. NeuroImage 80, 360–378.
Jann, K., Kottlow, M., Dierks, T., Boesch, C., Koenig, T., 2010. Topographic electrophysiological signatures of fMRI resting state networks. PLoS One 5, e12945.
Kaiser, R.H., Andrews-Hanna, J.R., Wager, T.D., Pizzagalli, D.A., 2015. Large-scale network dysfunction in major depressive disorder: a meta-analysis of resting-state functional connectivity. JAMA Psychiatr. 72, 603–611.
Kayser, S., Bewernick, B.H., Grubert, C., Hadrysiewicz, B.L., Axmacher, N., Schlaepfer, T.E., 2011. Antidepressant effects, of magnetic seizure therapy and electroconvulsive therapy, in treatment-resistant depression. J. Psychiatr. Res. 45, 569–576.
Kayser, S., Bewernick, B., Matusch, A., Hurlemann, R., Soehle, M., Schlaepfer, T.E., 2015. Magnetic seizure therapy in treatment-resistant depression: clinical, neuropsychological and metabolic effects. Psychol. Med. 45, 1073–1092.
Kennedy, S.H., Evans, K.R., Krüger, S., Mayberg, H.S., Meyer, J.H., McCann, S., et al., 2001. Changes in regional brain glucose metabolism measured with positron emission tomography after paroxetine treatment of major depression. Am. J. Psychiatr. 158, 899–905.
Khanna, A., Pascual-Leone, A., Farzan, F., 2014. Reliability of resting-state microstate features in electroencephalography. PLoS One 9, e114163.
Kho, K.H., van Vreeswijk, M.F., Simpson, S., Zwinderman, A.H., 2003. A meta-analysis of electroconvulsive therapy efficacy in depression. J. ECT 19, 139–147.
Kikuchi, M., Koenig, T., Wada, Y., Higashima, M., Koshino, Y., Strik, W., et al., 2007. Native EEG and treatment effects in neuroleptic-naive schizophrenic patients: time and frequency domain approaches. Schizophr. Res. 97, 163–172.
Kinoshita, T., Strik, W., Michel, C., Yagyu, T., Saito, M., Lehmann, D., 1995. Microstate segmentation of spontaneous multichannel EEG map series under diazepam and sulpiride. Pharmacopsychiatry 28, 51–55.
Koenig, T., Prichep, L., Lehmann, D., Sosa, P.V., Braeker, E., Kleinlogel, H., et al., 2002. Millisecond by millisecond, year by year: normative EEG microstates and developmental stages. NeuroImage 16, 41–48.
Kok, A., 1997. Event-related-potential (ERP) reflections of mental resources: a review and synthesis. Biol. Psychol. 45, 19–56.
Lehmann, D., Ozaki, H., Pal, I., 1987. EEG alpha map series: brain micro-states by space-

oriented adaptive segmentation. Electroencephalogr. Clin. Neurophysiol. 67, 271–288.
Lehmann, D., Faber, P.L., Galderisi, S., Herrmann, W.M., Kinoshita, T., Koukkou, M., et al., 2005. EEG microstate duration and syntax in acute, medication-naive, first-episode schizophrenia: a multi-center study. Psychiatry Res. Neuroimaging 138, 141–156.
Lisanby, S.H., Luber, B., Schlaepfer, T.E., Sackeim, H.A., 2003. Safety and feasibility of magnetic seizure therapy (MST) in major depression: randomized within-subject comparison with electroconvulsive therapy. Neuropsychopharmacology 28, 1852.
Mayberg, H.S., 2003. Modulating dysfunctional limbic-cortical circuits in depression: towards development of brain-based algorithms for diagnosis and optimised treatment. Br. Med. Bull. 65, 193–207.
Mayberg, H.S., Brannan, S.K., Mahurin, R.K., Jerabek, P.A., Brickman, J.S., Tekell, J.L., et al., 1997. Cingulate function in depression: a potential predictor of treatment response. Neuroreport 8, 1057–1061.
Menon, V., Uddin, L.Q., 2010. Saliency, switching, attention and control: a network model of insula function. Brain Struct. Funct. 214, 655–667.
Michel, C.M., Koenig, T., 2017. EEG microstates as a tool for studying the temporal dynamics of whole-brain neuronal networks: A review. NeuroImage 180, 577–593.
Milz, P., Faber, P.L., Lehmann, D., Koenig, T., Kochi, K., Pascual-Marqui, R.D., 2016a. The functional significance of EEG microstates—associations with modalities of thinking. NeuroImage 125, 643–656.
Milz, P., Pascual-Marqui, R.D., Lehmann, D., Faber, P.L., 2016b. Modalities of thinking: state and trait effects on cross-frequency functional independent brain networks. Brain Topogr. 29, 477–490.
Moscrip, T.D., Terrace, H.S., Sackeim, H.A., Lisanby, S.H., 2006. Randomized controlled trial of the cognitive side-effects of magnetic seizure therapy (MST) and electroconvulsive shock (ECS). Int. J. Neuropsychopharmacol. 9, 1–11.
Mulders, P.C., van Eijndhoven, P.F., Schene, A.H., Beckmann, C.F., Tendolkar, I., 2015. Resting-state functional connectivity in major depressive disorder: a review. Neurosci. Biobehav. Rev. 56, 330–344.
Musso, F., Brinkmeyer, J., Mobascher, A., Warbrick, T., Winterer, G., 2010. Spontaneous brain activity and EEG microstates. A novel EEG/fMRI analysis approach to explore resting-state networks. NeuroImage 52, 1149–1161.
Nobler, M.S., Oquendo, M.A., Kegeles, L.S., Malone, K.M., Campbell, C., Sackeim, H.A., et al., 2001. Decreased regional brain metabolism after ECT. Am. J. Psychiatr. 158, 305–308.
Pascual-Marqui, R.D., Michel, C.M., Lehmann, D., 1995. Segmentation of brain electrical activity into microstates: model estimation and validation. Biomed. Eng. IEEE Trans. 42, 658–665.
Pascual-Marqui, R.D., Lehmann, D., Koenig, T., Kochi, K., Merlo, M.C., Hell, D., et al., 1999. Low resolution brain electromagnetic tomography (LORETA) functional imaging in acute, neuroleptic-naive, first-episode, productive schizophrenia. Psychiatry Res. Neuroimaging 90, 169–179.
Pascual-Marqui, R.D., Lehmann, D., Faber, P., Milz, P., Kochi, K., Yoshimura, M., et al., 2014. The Resting Microstate Networks (RMN): Cortical Distributions, Dynamics, and Frequency Specific Information Flow. (arXiv preprint arXiv:14111949).
Perrin, F., Pernier, J., Bertrand, O., Echallier, J., 1989. Spherical splines for scalp potential and current density mapping. Electroencephalogr. Clin. Neurophysiol. 72, 184–187.
Perrin, J.S., Merz, S., Bennett, D.M., Currie, J., Steele, D.J., Reid, I.C., et al., 2012. Electroconvulsive therapy reduces frontal cortical connectivity in severe depressive disorder. Proc. Natl. Acad. Sci. 109, 5464–5468.
Rieger, K., Hernandez, L.D., Baenninger, A., Koenig, T., 2016. 15 years of Microstate research in schizophrenia–where are we? A Meta-analysis. Front. Psychiatr. 7.
Rodriguez, G., Vitali, P., De Leo, C., De Carli, F., Girtler, N., Nobili, F., 2002. Quantitative EEG changes in Alzheimer patients during long-term donepezil therapy. Neuropsychobiology 46, 49–56.
Rubinov, M., Sporns, O., 2010. Complex network measures of brain connectivity: uses and interpretations. NeuroImage 52, 1059–1069.
Sackeim, H.A., 1999. The anticonvulsant hypothesis of the mechanisms of action of ECT: current status. J. ECT 15, 5–26.
Sackeim, H.A., Luber, B., Katzman, G.P., Moeller, J.R., Prudic, J., Devanand, D., et al., 1996. The effects of electroconvulsive therapy on quantitative electroencephalograms: relationship to clinical outcome. Arch. Gen. Psychiatry 53, 814–824.
Sackeim, H.A., Prudic, J., Nobler, M.S., Fitzsimons, L., Lisanby, S.H., Payne, N., et al., 2008. Effects of pulse width and electrode placement on the efficacy and cognitive effects of electroconvulsive therapy. Brain Stimulation 1, 71–83.
Sanacora, G., Mason, G.F., Rothman, D.L., Hyder, F., Ciarcia, J.J., Ostroff, R.B., et al., 2003. Increased cortical GABA concentrations in depressed patients receiving ECT. Am. J. Psychiatr. 160, 577–579.
Santarnecchi, E., Khanna, A.R., Musaeus, C.S., Benwell, C.S., Davila, P., Farzan, F., et al., 2017. EEG microstate correlates of fluid intelligence and response to cognitive training. Brain Topogr. 30, 1–19.
Schwab, S., Koenig, T., Morishima, Y., Dierks, T., Federspiel, A., Jann, K., 2015. Discovering frequency sensitive thalamic nuclei from EEG microstate informed resting state fMRI. NeuroImage 118, 368–375.
Spellman, T., McClintock, S.M., Terrace, H., Luber, B., Husain, M.M., Lisanby, S.H., 2008. Differential effects of high-dose magnetic seizure therapy and electroconvulsive shock on cognitive function. Biol. Psychiatry 63, 1163–1170.
Stam, C., Jones, B., Nolte, G., Breakspear, M., Scheltens, P., 2006. Small-world networks and functional connectivity in Alzheimer's disease. Cereb. Cortex 17, 92–99.
Strik, W., Dierks, T., Becker, T., Lehmann, D., 1995. Larger topographical variance and decreased duration of brain electric microstates in depression. J. Neural Transm. 99, 213–222.
Sun, Y., Farzan, F., Mulsant, B.H., Rajji, T.K., Fitzgerald, P.B., Barr, M.S., et al., 2016. Indicators for remission of suicidal ideation following magnetic seizure therapy in patients with treatment-resistant depression. JAMA Psychiatr. 73, 337–345.
Tibshirani, R., Walther, G., 2005. Cluster validation by prediction strength. J. Comput. Graph. Stat. 14, 511–528.
Tomescu, M.I., Rihs, T.A., Becker, R., Britz, J., Custo, A., Grouiller, F., et al., 2014. Deviant dynamics of EEG resting state pattern in 22q11. 2 deletion syndrome adolescents: a vulnerability marker of schizophrenia? Schizophr. Res. 157, 175–181.
Tononi, G., Sporns, O., Edelman, G.M., 1994. A measure for brain complexity: relating functional segregation and integration in the nervous system. Proc. Natl. Acad. Sci. 91, 5033–5037.
Veer, I.M., Beckmann, C.F., Van Tol, M.-J., Ferrarini, L., Milles, J., Veltman, D.J., et al., 2010. Whole brain resting-state analysis reveals decreased functional connectivity in major depression. Front. Syst. Neurosci. 4.
Wang, L., Zhu, C., He, Y., Zang, Y., Cao, Q., Zhang, H., et al., 2009. Altered small-world brain functional networks in children with attention-deficit/hyperactivity disorder. Hum. Brain Mapp. 30, 638–649.
Guo, W., Sun, X., Liu, L., Xu, Q., Wu, R., Liu, Z., et al., 2011. Disrupted regional homogeneity in treatment-resistant depression: a resting-state fMRI study. Prog. Neuro-Psychopharmacol. Biol. Psychiatry 35, 1297–1302.
Whitfield-Gabrieli, S., Ford, J.M., 2012. Default mode network activity and connectivity in psychopathology. Annu. Rev. Clin. Psychol. 8, 49–76.
Wu, Q.Z., Li, D.M., Kuang, W.H., Zhang, T.J., Lui, S., Huang, X.Q., et al., 2011. Abnormal regional spontaneous neural activity in treatment-refractory depression revealed by resting-state fMRI. Hum. Brain Mapp. 32, 1290–1299.
Yamamura, T., Okamoto, Y., Okada, G., Takaishi, Y., Takamura, M., Mantani, A., et al., 2016. Association of thalamic hyperactivity with treatment-resistant depression and poor response in early treatment for major depression: a resting-state fMRI study using fractional amplitude of low-frequency fluctuations. Transl. Psychiatry 6, 1–9.
Yuan, H., Zotev, V., Phillips, R., Drevets, W.C., Bodurka, J., 2012. Spatiotemporal dynamics of the brain at rest—exploring EEG microstates as electrophysiological signatures of BOLD resting state networks. NeuroImage 60, 2062–2072.
Zhang, J., Wang, J., Wu, Q., Kuang, W., Huang, X., He, Y., et al., 2011. Disrupted brain connectivity networks in drug-naive, first-episode major depressive disorder. Biol. Psychiatry 70, 334–342.